JOURNAL OF QUATERNARY SCIENCE (2021) 1–16 ISSN 0267-8179. DOI: 10.1002/jqs.3290

JQS Journal of Quaternary Science QRA Quaternary Research Association

Not herbs and forbs alone: pollen-based evidence for the presence of boreal trees and shrubs in Cis-Baikal (Eastern Siberia) derived from the Last Glacial Maximum sediment of Lake Ochaul

FRANZISKA KOBE,[1] CHRISTIAN LEIPE,[1,2] ALEXANDER A. SHCHETNIKOV,[3,4,5,6,7] PHILIPP HOELZMANN,[8] JANA GLIWA,[9] PASCAL OLSCHEWSKI,[1,9] TOMASZ GOSLAR,[10,11] MAYKE WAGNER,[9] ELENA V. BEZRUKOVA[3,4] and PAVEL E. TARASOV[1]*

[1]Institute of Geological Sciences, Paleontology, Freie Universität Berlin, Berlin, Germany
[2]Institute for Space-Earth Environmental Research (ISEE), Nagoya University, Nagoya, Japan
[3]A.P. Vinogradov Institute of Geochemistry, Siberian Branch of Russian Academy of Sciences, Irkutsk, Russia
[4]Irkutsk Scientific Center, Siberian Branch of Russian Academy of Sciences, Irkutsk, Russia
[5]Institute of the Earth's Crust, Siberian Branch of the Russian Academy of Sciences, Irkutsk, Russia
[6]Geological Institute, Russian Academy of Sciences, Moscow, Russia
[7]Laboratory of Geoarchaeology of Baikal Siberia, Irkutsk State University, Irkutsk, Russia
[8]Institute of Geographical Sciences, Physical Geography, Freie Universität Berlin, Berlin, Germany
[9]Eurasia Department and Beijing Branch Office, German Archaeological Institute, Berlin, Germany
[10]Faculty of Physics, Adam Mickiewicz University, Poznań, Poland
[11]Poznan Radiocarbon Laboratory, Poznan Park of Science and Technology, Poznań, Poland

Received 4 December 2020; Revised 28 January 2021; Accepted 14 February 2021

ABSTRACT: A new accerator mass spectrometry (AMS)-dated sedimentary record from Lake Ochaul (54°14′N, 106°28′E; 641 m a.s.l.) in Eastern Siberia covers the interval from ca. 27 850 to 20 400 cal a BP at ca. 180-year resolution and contributes to a better understanding of the complex spatial vegetation pattern during the Last Glacial Maximum (LGM). Non-arboreal pollen taxa are abundant in the pollen assemblages (mean value ca. 92.6%), but boreal trees are represented by all major taxa that grow in the lake catchment today, including *Betula* sect. *Albae* (0.6–4.8%), *Picea* (0.6–2.8%), *Pinus sibirica* (*Haploxylon* type) (up to 1.5%), *Pinus sylvestris* (*Diploxylon* type) (up to 2%), *Larix* (up to 0.6%) and *Abies* (up to 0.6%). *Betula* sect. *Nanae/Fruticosae* (2–5.2%) and *Salix* (up to 3.2%) are the most representative boreal shrub taxa. Together with existing modern and fossil pollen data from the wider study region, the current record provides further evidence for the long-debated presence of boreal trees and shrubs in Eastern Siberia throughout the LGM. Our results show that the Upper Lena was a region in which refugia for arboreal taxa existed and that far-distant pollen transport can be ruled out as the source of the detected arboreal pollen.

KEYWORDS: arboreal pollen; biome reconstruction; ostracods; productive vegetation; sediment geochemistry

Introduction

The 21st century brings many environmental threats to forest ecosystems, including different forms of pollution, anthropogenic deforestation and mining activities. A quantitative assessment of global forest changes using Earth observation satellite data revealed forest loss of about 2.3 million km^2 from 2000 to 2012 (Hansen *et al.*, 2013). Their study also showed that the loss of boreal forests, mainly due to fires and logging, was comparable to that in the tropics in absolute and proportional terms. This trend is particularly alarming given slower regrowth dynamics of boreal conifer trees. Tautenhahn *et al.* (2016) reported that recent climate change and associated increase in fire frequency are also transforming the landscape in the boreal forest regions, and those transformations, in turn, will have an impact on the regional and global climate, which must be better understood.

Knowledge of past forest change helps to gain insight into the climate system, carbon cycle and genetic diversity, and can inform current predictions and conservation strategies (e.g. Prentice *et al.*, 1992; Petit *et al.*, 2008; Tarasov *et al.*, 2009; Williams *et al.*, 2011; Kaplan *et al.*, 2016). There is general agreement that the Earth's forests underwent substantial decline during the Quaternary glacial intervals (e.g. Melles *et al.*, 2012) and that the Last Glacial Maximum [LGM: ca. 30–18 cal ka BP (Lambeck *et al.*, 2014) or 26.5–20 cal ka BP (Clark *et al.*, 2009)] landscapes in the middle to high latitudes were predominantly treeless (Frenzel *et al.*, 1992; Prentice *et al.*, 2000; Williams *et al.*, 2011; Shao *et al.*, 2018) in response to the maximum spread of ice sheets and corresponding minima in global sea level, northern summer insolation, sea surface temperatures and atmospheric CO_2 concentrations. However, the extent of deforestation and characteristics of the LGM vegetation cover and climate in northern Asia (Fig. 1A), a region that witnessed continuous human habitation during the climatically harshest part of the last glacial (e.g. Fiedel and Kuzmin, 2007) and played a key role in the spread of anatomically modern humans to America, are still debated (e.g. Tarasov *et al.*, 2020).

Botanical records from ice-free high-latitude regions of Eurasia and North America indicate that boreal forests became rather quickly established there during the Lateglacial and the

*Correspondence: Pavel E. Tarasov, as above.
E-mail: ptarasov@zedat.fu-berlin.de

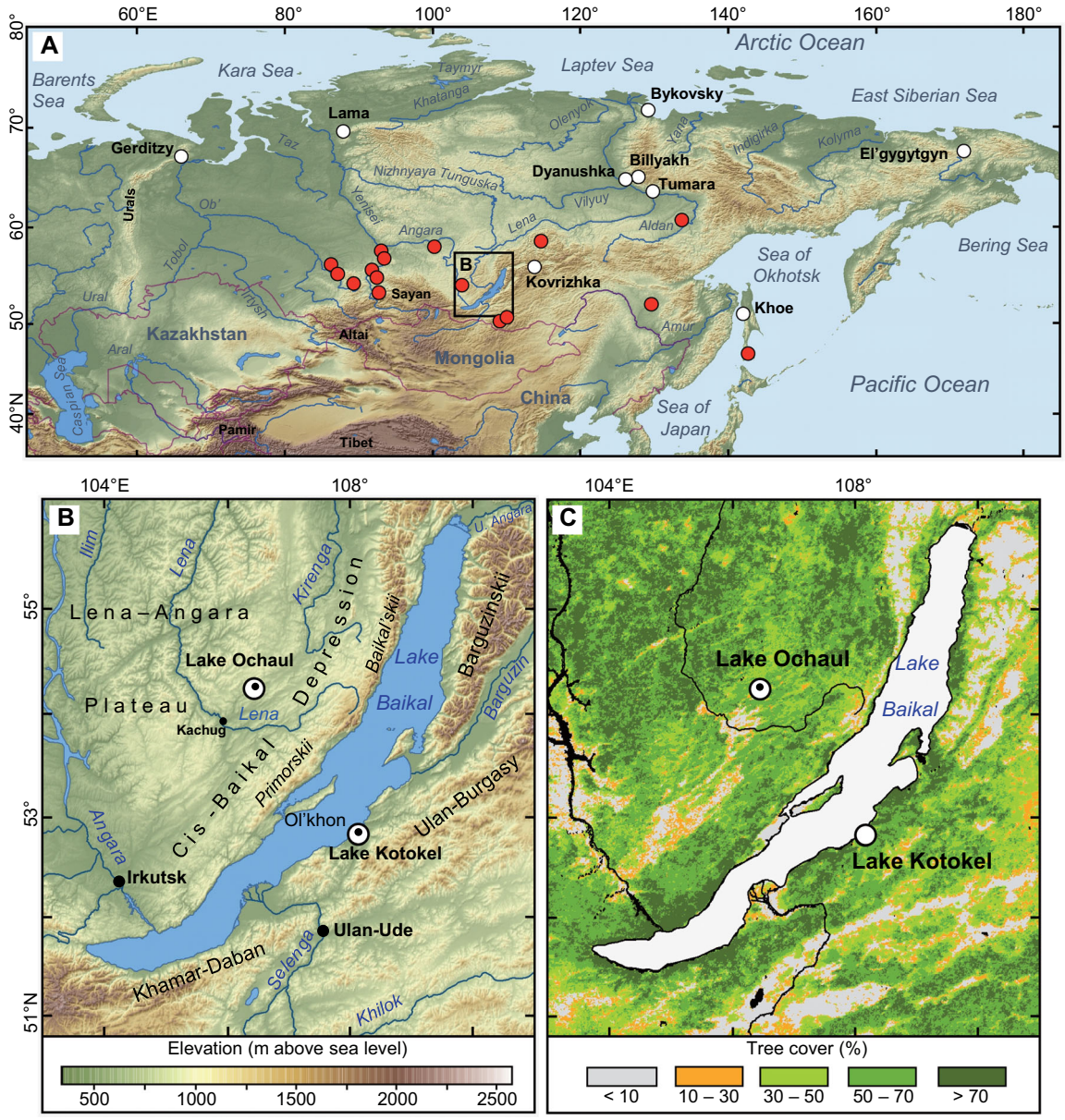

Figure 1. Maps showing: (A) locations of the Lake Baikal region (LBR: black rectangle) and the sites with published pollen or/and plant macrofossil records from northern Eurasia discussed in the text (white dots) and with radiocarbon-dated Last Glacial Maximum wood and charcoal material (red dots) from archaeological sites in Siberia and the Russian Far East (Vasil'ev *et al.*, 2002); (B) main topographic features, hydrological network, and locations of Lake Ochaul and Lake Kotokel in the LBR; and (C) AVHRR-derived percentage values of modern tree cover (DeFries *et al.*, 2000). Elevation in A and B is based on 90-m resolution Shuttle Radar Topography Mission (SRTM) v4.1 data (Jarvis *et al.*, 2008). [Color figure can be viewed at wileyonlinelibrary.com].

early Holocene interglacial because of population invasion from southern glacial refugia and local expansion of small tree populations that survived the LGM interval in cryptic refugia (Petit *et al.*, 2008). A multidisciplinary study of the Dyanushka peat section (Fig. 1A) from the Lena River valley (Werner *et al.*, 2010) reported well-preserved and radiocarbon-dated needles and cones of *Larix*, thus documenting local presence of larch trees 170 km south of the Arctic Circle during the Younger Dryas stadial (ca. 12 500–12 000 cal a BP). Furthermore, a sediment record from Lake Billyakh (Fig. 1A) situated in the Verkhoyansk Mountains, ca. 80 km east of the Dyanushka site, revealed almost continuous presence of larch pollen through the last 50 000 years (Müller *et al.*, 2010). Further evidence that small populations of woody taxa grew in climatically favourable habitats comes from radiocarbon-dated wood and charcoal material from archaeological sites in Southern Siberia (Fig. 1A; Vasil'ev *et al.*, 2002) and from ancient DNA (aDNA) analysis of stomach contents and coprolites of large herbivores dating ca. 55 000–21 000 cal a BP (Willerslev *et al.*, 2014). However, due to a lack of directly dated LGM wood macrofossils and high-resolution aDNA and pollen records from the central part of Eastern Siberia, there has been no agreement on whether (and, if so, where?) trees could persist during the coldest phases of the last glacial period (Frenzel *et al.*, 1992; Ray and Adams, 2001; Brubaker *et al.*, 2005; Binney *et al.*, 2009; Tarasov *et al.*, 2009). In the current study, we present a new accerator mass spectrometry (AMS)-dated pollen record supplemented by the results of geochemical and ostracod analyses of the LGM sediment from Lake Ochaul (Fig. 1B), situated in a densely forested taiga zone (Fig. 1C), to fill the gap in the current knowledge and address this problem.

Study site and environmental setting

Lake Ochaul (54°14′N, 106°28′E; 641 m a.s.l.) is a relatively small freshwater lake situated in the upper reaches of the Lena

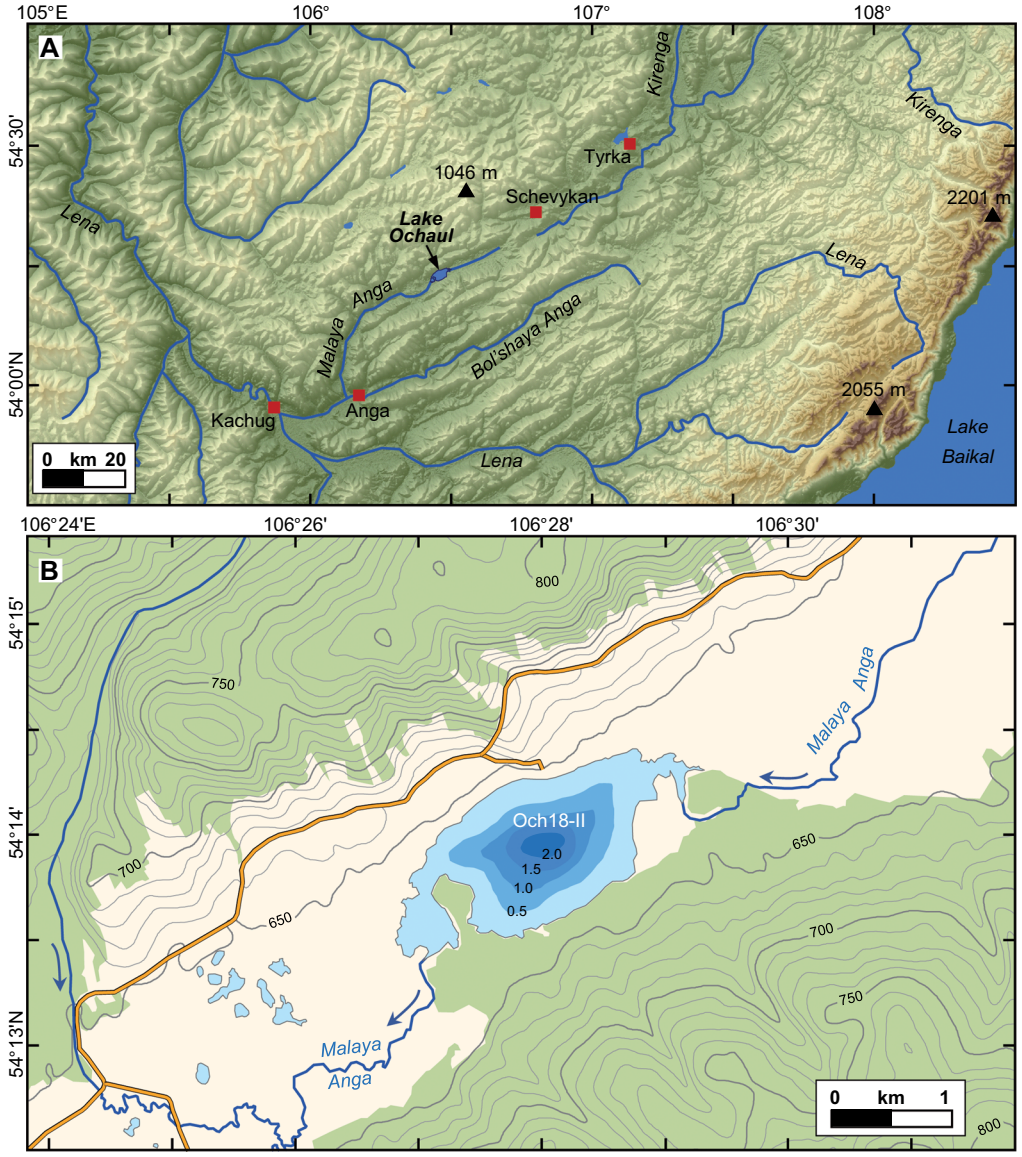

Figure 2. (A) The Malaya Anga River and Lake Ochaul catchment area in the Upper Lena region. Elevation is based on Jarvis *et al.* (2008). (B) Location of the Och18-II coring site and simplified bathymetry of Lake Ochaul (after https://ru.mapy.cz/ with modifications). The bathymetric survey was performed using a Humminbird HELIX 9 CHIRP GPS G4N echo sounder and chartplotter with a sonar frequency of 83/200/455 kHz. [Color figure can be viewed at wileyonlinelibrary.com].

River, about 100 km north-west of Lake Baikal (Fig. 2A). Ochaul located in the Upper Lena region, rich in archaeological sites assigned to the Upper Palaeolithic, Neolithic and Bronze Age periods, was selected as one of the key study sites for a new phase of the Baikal Archaeology Project (BAP), a long-term interdisciplinary research project focused on detailed reconstructions of hunter-gatherer culture and environmental dynamics (Weber *et al.*, 2013; https://baikalproject.artsrn.ualberta.ca/). The lake has a maximum length of ca. 2.7 km, a maximum width of ca. 1.2 km and a water surface area of ca. 2.6 km^2 (Boyarkin, 2007). The lake is rather shallow (Fig. 2B) and its bottom is overgrown with aquatic vegetation. A maximum water depth measured in summer 2018 in the central part of the lake was about 2.5 m, although traces of 2–3-m-high palaeoshorelines observed in the eastern part of the lake, ca. 100–300 m from its modern coastline, indicate that the lake occupied a larger area at some time in the past (Kobe *et al.*, 2020). Dating these former shorelines may contribute to a better understanding of the lake history. However, due to the archaeological sites located on the lake shore, any geomorphological field work is prohibited.

Lake Ochaul (Fig. 2B) occupies the central part of a trough-shaped valley with a flat and marshy bottom and slopes rising to 200–250 m above the lake level (i.e. 850–900 m a.s.l.). The Malaya Anga River, flowing through the lake, carries its waters to the Bol'shaya Anga, which flows into the Lena River near Kachug (Fig. 2A), a small town and county centre, founded in 1686.

The valleys of the Malaya and Bol'shaya Anga rivers are part of the larger Cis-Baikal Depression (Kobe *et al.*, 2020), which stretches parallel to Lake Baikal from the Angara River in the south-west to the Kirenga River in the north-east (Fig. 1B) and has a tectonic origin (Alpat'ev *et al.*, 1976). The Primorskii (1658 m a.s.l.) and the Baikal'skii (2588 m) mountain ranges separate the depression from Lake Baikal, while the Lena–Angara Plateau borders it from the north-west. The bedrocks of the lake drainage area are represented by sedimentary rocks of the Middle–Upper Cambrian Verkholenskaya suite, including dolomite marls, often with anhydrite, gypsum, as well as mudstones, siltstones and sandstones (Vinogradov *et al.*, 2011). The reddish-brownish colours of the underlying rocks are transmitted in the process of lithogenesis

to the overlying Cenozoic sediments, primarily on the slopes and in the lake basins.

The regional climate is continental with relatively warm but short summers and cold long winters (Alpat'ev *et al.*, 1976). The climate averages from Kachug show a mean temperature of −25.5 °C in January, 17.1 °C in July, an annual precipitation of 339 mm (https://ru.climate-data.org/) and a period of continuous snow cover of 167 days (Galaziy, 1993; Kobe *et al.*, 2020). In contrast to the low precipitation values registered in the Cis-Baikal Depression, the neighbouring mountain ranges receive up to 1000–1200 mm annually (Galaziy, 1993). This and low evaporation losses explain the well-developed river network of the region (Fig. 2A).

The study region belongs to the southern and species-richest part of the taiga vegetation zone of Eastern Siberia (Alpat'ev *et al.*, 1976) and the plain areas outside the human settlements and mountains are densely forested (Fig. 1C). The regional vegetation is dominated by deciduous [e.g. larch (*Larix* sp.) and birch (*Betula* sect. *Albae*)] and evergreen [e.g. Siberian pine (*Pinus sibirica*), Scots pine (*Pinus sylvestris*), spruce (*Picea obovata*) and fir (*Abies sibirica*)] trees. The undergrowth is represented by diverse shrubs, including heath (*Ledum palustre*, *Vaccinium vitis-idaea*, *V. uliginosum*), alder (*Alnus fruticosa*), willow (*Salix* sp.) and birch (*Betula* sect. *Fruticosae* and *B.* sect. *Nanae*) as well as various herb, grass and moss species (Belov *et al.*, 2002). In the catchment area of Lake Ochaul, larch forests with admixture of Siberian pine, spruce and birch trees and with abundant birch shrubs in the undergrowth dominate (Belov *et al.*, 2002; Kobe *et al.*, 2020), while Scots pines are not as common as in the other regions, e.g. Trans-Baikal, the Angara River valley and Central Yakutia (Alpat'ev *et al.*, 1976), where subsurface permafrost is not affecting their root system (Shumilova, 1960). Large elevation differences (i.e. 455–2201 m a.s.l.) and complex topography in the study region (Fig. 2A) cause very variable climatic and micro-climatic conditions (Galaziy, 1993), which explain the patchy character of vegetation distribution and high diversity of plants (Belov *et al.*, 2002) representing different vegetation types or biomes such as taiga, cold deciduous forest, steppe and tundra (Demske *et al.*, 2005; Tarasov *et al.*, 2019; Kobe *et al.*, 2020).

Materials and methods

Core sediment and age determination

Lake Ochaul was cored in summer 2018 using a UWITEC percussion piston corer and coring platform (Kobe *et al.*, 2020). The sediment core Och18-II (Fig. 3) was retrieved from the central part of the lake (54°13′58.4″N, 106°27′53.8″E; Fig. 2B) at a water depth of ca. 2.5 m. Once coring was completed, the core sections in closed thin-wall plastic liners of 63-mm diameter were transported to the Institute of Geochemistry, Siberian Branch of the Russian Academy of Sciences in Irkutsk and stored under constantly low temperature. In March 2019, the tubes were opened by cutting in two halves, the sediments were photographed, described, documented and subsampled for further analyses using the double-L channel (LL-channel) technique (Nakagawa, 2007).

The Och18-II core revealed a 7.24-m-long sediment column (Kobe *et al.*, 2020), which consists of two major units. The topmost one (0–213 cm) is represented by water-rich soft organic gyttja, rich in freshwater mollusc and ostracod shells, partly laminated, coloured in various shades of brown (Fig. 3B), with a pungent smell of hydrogen sulphide (Kobe *et al.*, 2020). A transitional layer of gyttja and laminated silty clay of olive-grey to blackish colour separates it from the underlying thick unit (236–724 cm) represented by massive viscous silty clay, partly finely laminated, light grey to dark grey in colour in the upper part, and reddish to brown massive viscous clay with coarse silt and fine sand in the bottom part of the core (Fig. 3B).

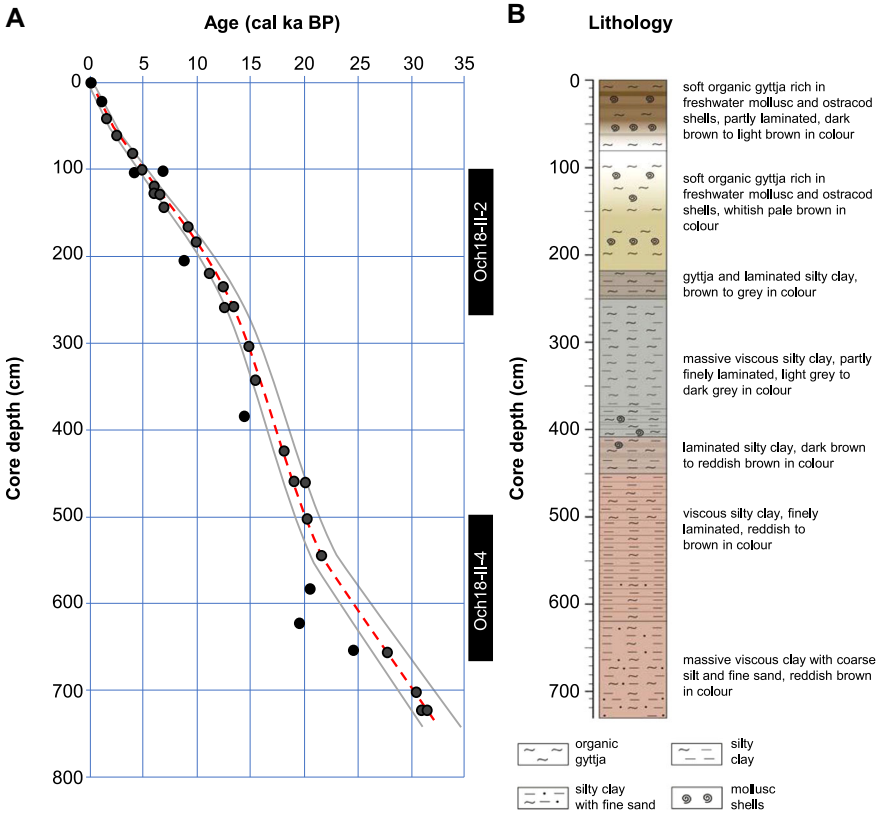

Figure 3. (A) AMS ^{14}C-based age-depth model and (B) simplified lithology of the Och18-II sediment core. Black dots indicate medians of calibrated radiocarbon dates corrected for reservoir effect (see Table 1 for details). Grey lines in A indicate ±5% uncertainty range of the age model (dashed red line). Vertical black bars indicate section 4 (this study) and section 2 (Kobe *et al.*, 2020) of the Och18-II core. [Color figure can be viewed at wileyonlinelibrary.com].

Table 1. Summary of radiocarbon dates, and calibrated and modelled ages for the set of 35 AMS-dated sediment samples from the Och18–II core of Lake Ochaul. Calibration was performed using OxCal v4.3 (Bronk Ramsey 1995) and the calibration curve IntCal20 (Reimer *et al.*, 2020).

Core segment ID	Radiocarbon laboratory number	Core composite depth (cm)	Radiocarbon date (^{14}C a BP)	Corrected radiocarbon date (^{14}C a BP)	95% age range (cal a BP)	Modelled age (cal a BP)
Och18/II-1	Poz-106375	0–1	615 ± 30	15 ± 30	255–34	−47
Och18/II-1	Poz-114424	1–2	695 ± 30	95 ± 30	265–22	−6
Och18/II-1	Poz-114366	21–22	1855 ± 30	1255 ± 30	1280–1074	815
Och18/II-1	Poz-114367	41–42	2310 ± 30	1710 ± 30	1699–1535	1637
Och18/II-1	Poz-114409	61–62	3110 ± 30	2510 ± 30	2735–2490	2459
Och18/II-1	Poz-114410	81–82	4255 ± 35	3655 ± 35	4090–3877	3281
Och18/II-1	Poz-114411	101–102	4940 ± 30	4340 ± 30	5021–4844	4102
Och18/II-1	Poz-114412	127–128	5815 ± 30	5215 ± 30	6165–5910	6215
Och18/II-1	Poz-106373	129–130	6140 ± 40	5540 ± 40	6404–6280	6374
Och18/II-2	Poz-106374	100–101	6440 ± 40	5840 ± 40	6745–6502	4062
Och18/II-2	Poz-114413	104–105	4430 ± 30	3830 ± 30	4405–4101	4180
Och18/II-2	Poz-114415	124–125	5930 ± 35	5330 ± 35	6263–5996	5971
Och18/II-2	Poz-114416	144–145	6655 ± 35	6055 ± 35	6996–6797	7495
Och18/II-2	Poz-114417	164–165	8790 ± 50	8190 ± 50	9287–9015	8821
Och18/II-2	Poz-114571	184–185	9550 ± 50	8950 ± 50	10 225–9914	9994
Och18/II-2	Poz-114518	204–205	8630 ± 50	8030 ± 50	9031–8658	11 047
Och18/II-2	Poz-114419	218–219	10 410 ± 50	9810 ± 50	11 317–11 166	11 724
Och18/II-2	Poz-114420	237–238	11 070 ± 50	10 470 ± 50	12 562–12 135	12 577
Och18/II-2	Poz-114421	258–259	12 180 ± 50	11 580 ± 50	13 540–13 291	13 443
Och18/II-2	Poz-106902	259–260	11 340 ± 60	10 740 ± 60	12 810–12 620	13 470
Och18/II-3	Poz-114422	304–304.5	13 130 ± 60	12 530 ± 60	15 121–14 360	14 762
Och18/II-3	Poz-114437	344–344.5	13 540 ± 70	12 940 ± 70	15 695–15 255	15 917
Och18/II-3	Poz-114423	384–384.5	12 950 ± 60	12 350 ± 60	14 841–14 102	17 072
Och18/II-3	Poz-114440	424–424.5	15 460 ± 80	14 860 ± 80	18 289–17 924	18 227
Och18/II-3	Poz-114441	459–459.5	16 480 ± 80	15 880 ± 80	19 415–18 953	19 237
Och18/II-3	Poz-106973	461–462	17 310 ± 100	16 710 ± 100	20 450–19 925	19 302
Och18/II-4	Poz-114442	504–505	17 450 ± 90	16 850 ± 90	20 570–20 060	20 544
Och18/II-4	Poz-114443	544–545	18 460 ± 100	17 860 ± 100	21 917–21 330	21 699
Och18/II-4	Poz-114444	584–585	17 640 ± 90	17 040 ± 90	20 826–20 280	23 888
Och18/II-4	Poz-114445	624–625	16 850 ± 80	16 250 ± 80	19 906–19 389	26 076
Och18/II-4	Poz-114439	654–655	21 090 ± 120	20 490 ± 120	25 100–24 296	27 717
Och18/II-4	Poz-106972	656–657	24 140 ± 170	23 540 ± 170	27 946–27 416	27 827
Och18/II-5	Poz-114487	702–703	26 810 ± 230	26 210 ± 230	30 960–30 065	30 343
Och18/II-5	Poz-114488	722–724	27 360 ± 240	26 760 ± 240	31 231–30 381	31 465
Och18/II-5	Poz-106975	723.5–724.5	28 180 ± 250	27 580 ± 250	32 003–31 130	31 519

To estimate the age of the Och18-II core, 35 bulk sediment samples, each representing a 0.5- or 1-cm sediment layer, were sent to the Poznan Radiocarbon Laboratory for AMS dating (Fig. 3A; Table 1). The obtained dates suggest accumulation of the recovered core sediment during the past ca. 32 000 years (Kobe *et al.*, 2020) and helped to select the 157-cm-long section 4 of the Och18-II core (further called Och18-II-4), which represents the composite depth interval between 657 and 500 cm (Fig. 3), for detailed pollen and geochemical analyses of the LGM, discussed in the current study. The first study on the Och18-II core (Kobe *et al.*, 2020), which focused on the Lateglacial and the early and middle Holocene interval (ca. 13 500–4000 cal a BP), suggested that the reservoir effect could be a problem in Lake Ochaul, based on the AMS dating of the topmost sample from the Och18-II core to 615 ± 30 ^{14}C a BP and the modern age of this sample obtained using down-core profiles of short-lived ^{210}Pb and ^{137}Cs isotopes. Following Kobe *et al.* (2020), we subtracted the reservoir age of 600 years from all radiocarbon dates before their calibration to calendar ages using OxCal v4.3 (https://c14.arch.ox.ac.uk/oxcal.html; Bronk Ramsey, 1995) and the IntCal20 curve (Reimer *et al.*, 2020). Using a constant correction value of 600 years for the entire core gave reasonable results. A distinct phase in the regional vegetation development, which is characterized by a noticeable decrease in the pollen content of boreal trees and a parallel increase in the percentages of boreal shrubs in the Och18-II-2 sediment section (Fig. 3A), was dated to ca. 12 650–11 650 cal a BP, which corresponds well to the Younger Dryas stadial (Kobe *et al.*, 2020). The obtained age model (Fig. 3A; Table 1) was applied to the Och18-II-4 records presented in the current study (see also Supporting Information Tables S1 and S2).

Sediment properties

Laboratory analyses of the physical and geochemical properties of sediment samples from the Och18-II-4 core section (Fig. 3) were performed at the Institute of Geographical Sciences (FU Berlin) and at the Institute of Geochemistry (SB RAS, Irkutsk). In the process of sample preparation for grain-size measurements, chemical pretreatment was done to isolate discrete particles of the sample from organic and carbonate cements and to provide an evenly dispersed suspension of individual particles (see Sun *et al.*, 2002 for details of the treatment procedure and references). Organic matter was dissolved with a 10% solution of H_2O_2 (Allen and Thornley, 2004; Mikutta *et al.*, 2005). The samples placed in test tubes were centrifuged for 15 min at 3000 r.p.m., then hydrogen peroxide was removed, distilled water was added and the process was repeated. Finally, the samples were dried at 105 °C.

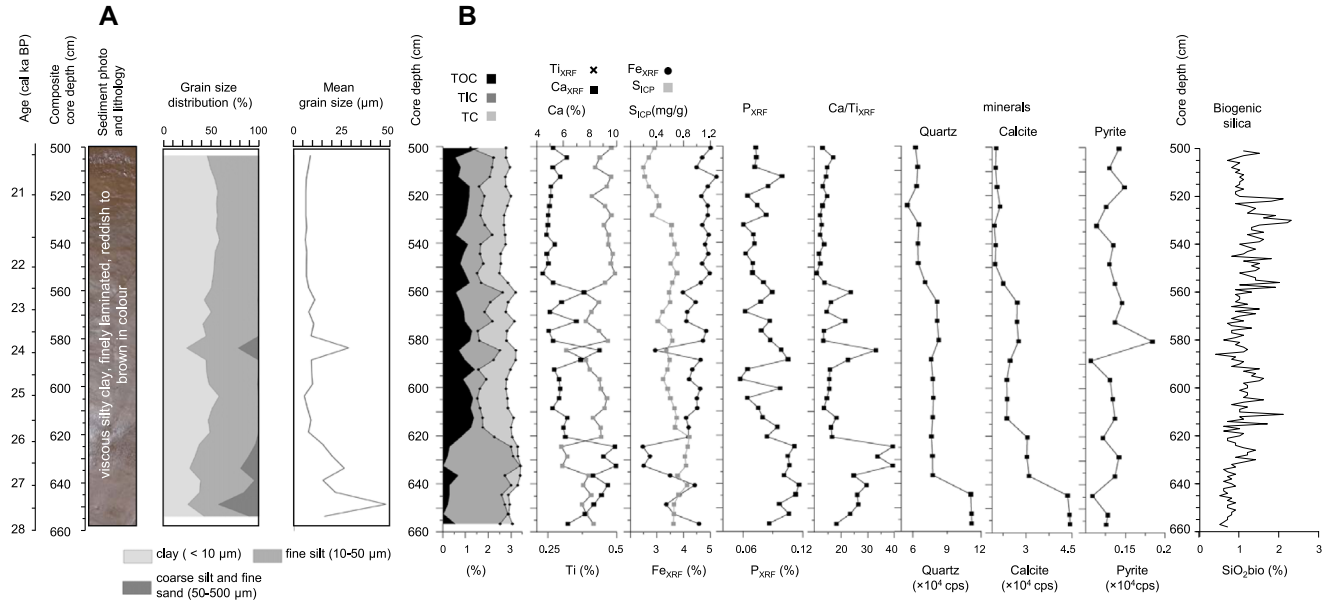

Figure 4. Summary of the Och18-II-4 sediment lithology (A) and geochemistry (B). [Color figure can be viewed at wileyonlinelibrary.com].

Particle size analysis (Fig. 4) was performed using a Fritsch Analysette 22 laser diffraction particle analyser equipped with an ultrasonic bath. The measurements were carried out before and after exposure to ultrasound (the latter measurements are presented here). The particles identified on the laser diffraction analyser were combined into the following groups: <10 μm (clay), 10–50 μm (fine silt) and >50 μm (coarse silt). The fraction of fine-grained sand (0.2–0.5 mm) was determined by standard sieving. This fraction in the samples did not exceed 1.5% or was completely absent. Therefore, it was combined with the coarse silt fraction (Fig. 4). Biogenic silica (SiO_2bio) was also measured at 1-cm intervals (Fig. 4) as described in Mortlock and Froelich (1989). Basic geochemical parameters such as elemental analysis of total carbon (TC), total inorganic carbon (TIC), total organic carbon (TOC) and total nitrogen (TN) as well as determination of sulphur (Fig. 4; Table S2) by ICP-OES (inductively coupled plasma optical emission spectrometry) on the base of an aqua regia extraction (DIN EN 2001) as well as portable energy-dispersive X-ray fluorescence spectrometry (P-ED XRF) with an Analyticon NITON XL3t of ground and homogenized samples were conducted for all selected samples. The main mineralogical components were determined by XRD (X-ray diffraction). The XRD results (Fig. 4) are expressed in counts per second (cps), which reflects semiquantitatively the proportion of the minerals. These common analyses are described in detail in Vogel *et al.* (2016).

Ostracod analysis

For the analysis of ostracods, six sediment samples (about 4 g dry weight), each representing a 1-cm-thick slice, have been taken from the Och18-II-4 core segment in 30-cm intervals (see Table 3). The samples were prepared for ostracod extraction, to test the potential for further in-depth ostracod analysis and to gain an overview of the taxonomic distribution and diversity during the investigated time interval. For the ostracod extraction, the samples were treated with H_2O_2 (10%) for several minutes to 4 h (depending on the reaction velocity) and wet-sieved with a mesh width of 106 μm under running tap water. Samples were freeze-dried afterwards and ostracods were hand-picked with a fine brush. For species identification, ostracods were sputtered with gold and photographed using a Leica S430 scanning electron microscope at the German Archaeological Institute. Species were identified with the ostracod determination keys published by Meisch (2000) and species descriptions in Bronstein (1947) and Mazepova (1990).

Pollen extraction, identification and visualization

Altogether, 40 sediment samples (each representing a 1-cm-thick slice) were taken in 4-cm steps from the 157-cm-long section 4 of the Och-18-II core with a weight of 2 g each. One tablet with exotic *Lycopodium* marker spores was added to each sample before chemical treatment to calculate the pollen and other palynomorph concentrations (Stockmarr, 1971).

Following the Sustainability Mission Statement adopted by the Freie Universität Berlin (FU Berlin) in research and teaching as well as EU regulations requiring the substitution of hazardous chemicals such as HF, we applied the extraction method protocol described by Leipe *et al.* (2019). All samples were first treated with 10% HCl to remove carbonates and to dissolve the calcareous matrix of the *Lycopodium* tablets, followed by a 10% KOH treatment in a hot water bath to remove humic acids. After removing clayey particles using low-speed centrifugation, dense media separation using sodium polytungstate (SPT) at a density of 2.1 g cm^{-3} to remove siliceous matter and other heavier particles was applied. After SPT treatment and following acetolysis, the sample residues were washed three times with distilled water and mounted in glycerol for conservation and microscopic analysis.

Pollen and non-pollen palynomorphs (NPPs) were counted using a light microscope with ×400 magnification and taxonomically identified with the help of published atlases (Reille, 1992, 1995, 1998; van Geel, 1978, 2001; Beug, 2004; Demske *et al.*, 2013; Savelieva *et al.*, 2013) and the Section of Paleontology FU Berlin reference collection. Counted pollen sums vary from 313 to 527 terrestrial pollen grains (372 on average) per sample.

In most cases, preservation of palynomorphs was sufficient for identification; however, in some cases tricolpate/tricolporate type pollen grains were corroded and could not be accurately assigned to a certain taxon (i.e. Brassicaceae, Saxifragaceae or Scrophulariaceae). They make up 1–5% of

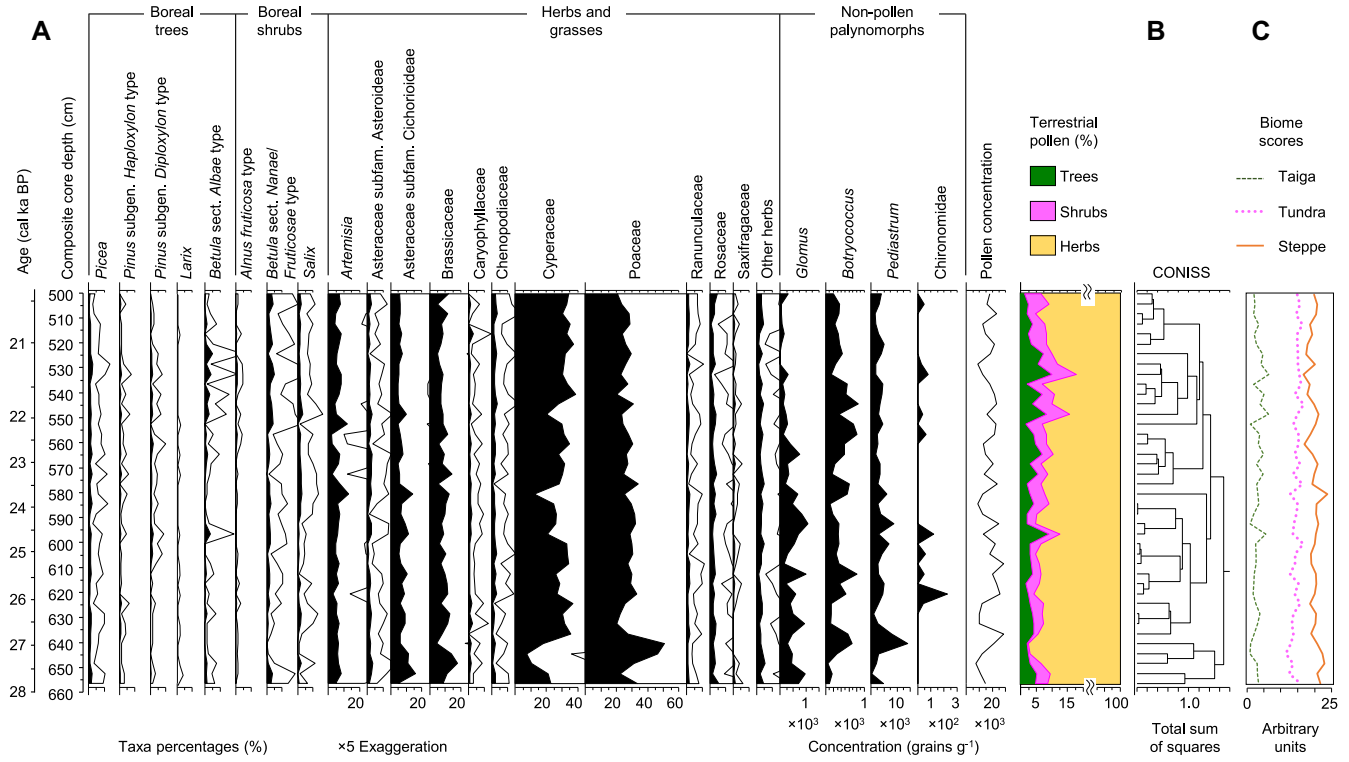

Figure 5. (A) Simplified diagram showing relative percentages of the most abundant arboreal and non-arboreal taxa, along with the concentration values of the representative non-pollen palynomorphs (NPPs); (B) the CONISS dendrogram; and (C) the pollen-derived biome scores of the Och18-II-4 record from Lake Ochaul plotted against the core depth and age axes. [Color figure can be viewed at wileyonlinelibrary.com].

the total pollen sum and are presented under the name 'Other herbs' in the pollen diagram (Fig. 5A). When distinguishing between pollen produced by birch trees (i.e. *Betula* sect. *Albae* type) and birch shrubs (i.e. *Betula* sect. *Nanae/Fruticosae* type), we used morphological criteria such as pollen grain size, wall thickness and pore size following Mäkelä (1996) and references therein. When distinguishing pollen of *Pinus* subgenus *Diploxylon* type (i.e. *P. sylvestris*) from *P.* subgenus *Haploxylon* type (i.e. *P. sibirica* and *P. pumila*) in the study region, we applied the morphological criteria presented in Beug (2004) and Nakagawa *et al.* (2000).

Percentage values for all terrestrial pollen taxa were calculated based on the sum of arboreal pollen (AP) and non-arboreal pollen (NAP) taken as 100%. Percentages for aquatic plant and terrestrial cryptogam taxa were calculated based on the terrestrial pollen sum plus the sum of palynomorphs in the corresponding group. NPPs are presented as absolute concentration values. Tilia version 1.7.16 software (Grimm, 2011) was used for calculating taxon percentages and drawing the diagram (Fig. 5A). The Tilia-associated CONISS program for stratigraphically constrained cluster analysis by the method of incremental sum of squares (Grimm, 1987) was used for checking potential pollen zone boundaries (Fig. 5B).

Vegetation reconstruction

An objective method for the assignment of pollen spectra to appropriate major vegetation types or biomes on the basis of the modern ecology, bioclimatic tolerance and geographical distribution of pollen-producing plants was first introduced by Prentice *et al.* (1996) and then successfully used in several global-scale international projects including the BIOME6000 vegetation mapping project (e.g. Prentice and Jolly, 2000) and the Paleoclimate Modelling Intercomparison Project (e.g. Kageyama *et al.*, 2001). The robustness of this quantitative approach was verified in different regional studies using representative surface pollen datasets from Siberia and from the vast areas around Lake Baikal (Edwards *et al.*, 2000; Müller *et al.*, 2010; Tarasov *et al.*, 1998b, 2005, 2013a; Binney *et al.*, 2017). Successful tests of the method allowed its application for reconstructing the interglacial vegetation dynamics in the Lake Baikal Region (LBR) over the past 500 000 years (Tarasov *et al.*, 2005, 2007; Prokopenko *et al.*, 2010). However, reconstructions of the LGM biomes and vegetation cover in northern Asia (Tarasov *et al.*, 2000; Williams *et al.*, 2011) and in the LBR (Bezrukova *et al.*, 2010; Müller *et al.*, 2014; Tarasov *et al.*, 2019) are of particular interest for the current study.

Recently, Kobe *et al.* (2020) applied the biome reconstruction approach to the Lateglacial and early to middle Holocene pollen record of the Och-18-II core to discuss the post-glacial vegetation dynamics around Lake Ochaul. Following Kobe *et al.* (2020), all terrestrial pollen taxa identified in Och18-II-4 were assigned to the corresponding regional biomes. Among them only 31 taxa, which exceed the universal threshold of 0.5% suggested by Prentice *et al.* (1996), influenced the biome reconstruction (Table 2). Calculations of the biome scores were performed in PPP Base (Guiot and Goeury, 1996). Square root transformation was applied to the pollen percentage values to increase the importance of minor pollen taxa. The biome with the highest affinity score or the one defined by a smaller number of plant functional types (when scores of several biomes are equal) is assigned to each pollen spectrum (Prentice *et al.*, 1996).

Results

Core chronology

A total of 35 radiocarbon dates were obtained on the samples from the Och18-II core (Table 1). After correction of the reservoir effect and calibration, these dates result in calendar ages between 0 and 32 000 cal a BP (Table 1). The age model

Table 2. Terrestrial pollen taxa, exceeding 0.5% universal threshold (Prentice *et al.*, 1996), identified in the late Quaternary pollen records from Lake Kotokel (Tarasov *et al.*, 2009; Bezrukova *et al.*, 2010; Müller *et al.*, 2014) and Lake Ochaul (Kobe *et al.*, 2020; this study) in the Lake Baikal region and their assignments to the respective biomes.

Biome	Taxa included
Tundra	*Alnus fruticosa*, *Betula* sect. *Nanae/Fruticosae*, Cyperaceae, Ericales, Poaceae, *Polemonium*, *Polygonum*, *Rumex*, *Salix*, Saxifragaceae, *Valeriana*
Cold deciduous forest	*Alnus* (tree), *Betula* sect. *Albae*, Ericales, *Larix*, *Pinus sylvestris* (subgen. *Diploxylon* type), *P. pumila* (subgen. *Haploxylon* type), *Salix*
Taiga	*Abies sibirica*, *Alnus* (tree), *Betula* sect. *Albae*, Ericales, *Larix*, *Picea obovata*, *Pinus sylvestris* (subgen. *Diploxylon* type), *P. sibirica* (subgen. *Haploxylon* type), *Ribes*, *Salix*
Cool conifer forest	*Abies sibirica*, *Alnus* (tree), *Betula* sect. *Albae*, Ericales, *Corylus*, *Larix*, *Picea obovata*, *Pinus sylvestris*, *P. sibirica* (subgen. *Haploxylon* type), *Ribes*, *Salix*, *Ulmus*
Steppe	Apiaceae, *Artemisia*, Asteraceae subfam. Asteroideae, A. subfam. Cichorioideae, Brassicaceae, Cannabaceae, Caryophyllaceae, Chenopodiaceae, Fabaceae, Lamiaceae, Liliaceae, *Plantago*, Poaceae, *Polygonum*, Ranunculaceae, Rosaceae, Rubiaceae, *Rumex*, Scrophulariaceae, *Thalictrum*, *Urtica*, *Valeriana*
Desert	*Artemisia*, Boraginaceae, Chenopodiaceae, *Ephedra*, *Polygonum*

(Fig. 3A) supports continuous sedimentation over this period and shows a fairly clear age–depth relationship despite several well-distinguishable outliers of unknown origin. The age–depth relationship for the Och18-II-4 section discussed in this study was calculated using two linear interpolation functions: $y = 54.708x - 8089.4$ (depth below 544.5 cm) and $y = 28.874x + 5977$ (depth above 544.5 cm), where y indicates the estimated age (in cal a BP) of the analysed sample at depth x (in cm) in the composite core. The accumulation rates are relatively low, i.e. about 2.3 cm of sediment in 100 years (on average). The Och18-II-4 section analysed in this paper dates to the interval between ca. 27 850 and 20 400 cal a BP. The accumulation rate in this part of the core is slightly lower than average, i.e. about 2.1 cm of sediment in 100 years.

Sediment properties

The section Och18-II-4 analysed in this study is composed of viscous silty clay, finely laminated, reddish to brown in colour (Fig. 4A). The TC contents (Fig. 4B) show similar values around 2.9% throughout the section. The TOC values vary around 1.0% between 625 and 500 cm. For the basal part of the section (656–630 cm) the TOC values are slightly lower (0.5%) and consequently the TIC content here is slightly higher (2.4%). The main minerogenic component is quartz (SiO_2) that dominates throughout the section. Calcite ($CaCO_3$) is the second most frequent mineral and decreases (according to the TIC contents) from ca. 23% in the lower part of the record (657–625 cm) to 15% in the upper part (625–500 cm). Pyrite (FeS_2) is present throughout the section and shows slightly elevated cps values between 580 and 500 cm. Other identified minerogenic components are phyllosilicates (muscovite $[KAl_2(Si_3Al)O_{10}(OH)_2]$ and chlorite $[Mg_xAl_xCr_xAl_xSi_{x4-}O_{10}(O)_8)]$) and silicates (albite $[Na(AlSi_3O_8)]$ as feldspar and amphibole $[Al_xCa_xFe_xK_xMg_xNa_xSiO_{22}(OH)_4]$) that all are present throughout the section. SiO_2bio percentages (Fig. 4B) are minimal (ca. 0.5%) near the base of the section, but show an increase up to ca. 2% in the middle (620–595 cm) and upper part (560–520 cm) of the record.

Ostracods

Ostracod shells were found in all six analysed samples, well representing the entire analysed section. In total, five different taxa were identified (Fig. 6). The number of counted ostracod specimens varies from six to 500 valves per sample (Table 3). *Cytherissa lacustris* is the most common species that has been found in all analysed samples, except the lowermost one from 656 to 655 cm depth. This sample is characterized by a very low abundance (six specimens), but relatively high diversity of ostracods (i.e. three species of the subfamily Candoninae) and the occurrence of broken valves. The samples from 628–627, 598–597 and 568–567 cm depth show monospecific assemblages with *C. lacustris*, while in the upper two samples (538–537 and 508–507 cm) *C. lacustris* is found in association with another species of *Candona*. All analysed samples, except the lowest one, show occurrences of juvenile specimens of at least three moulting stages.

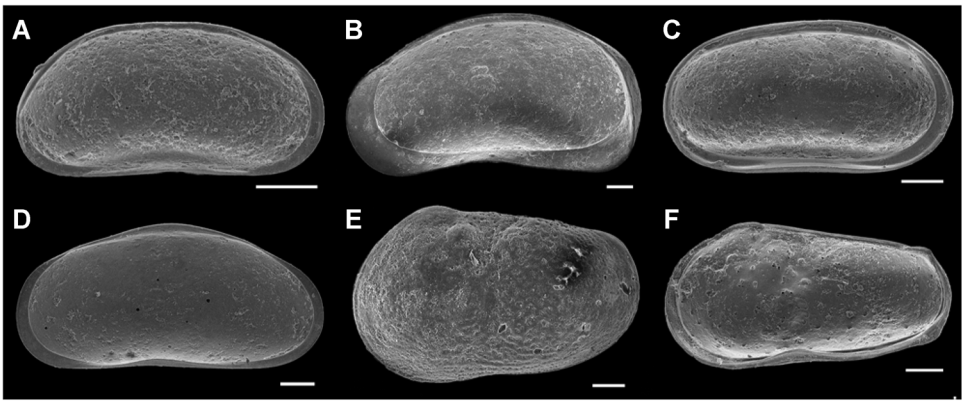

Figure 6. Ostracod specimens extracted from sediment samples of Och18-II-4: (A) *Candona* sp. 1, left valve, internal view; (B) *Candona* sp. 2, right valve, internal view; (C) Candoninae indet., left valve, internal view; (D) *Candona* sp. 3, right valve, internal view; (E–F) *Cytherissa lacustris* Sars 1863: (E) female, left valve, external view, (F) male, right valve, internal view. Scale bars represent 100 µm.

Table 3. Results of ostracod analysis of six sediment samples from the Och18-II-4 section.

	Sample depth (cm)					
Taxon name	507–508	537–538	567–568	597–598	627–628	655–656
Candona sp. 1						1
Candona sp. 2						3
Candoninae indet.						2
Candona sp. 3	14	230				
Cytherissa lacustris	12	13	208	61	500	
Total counted valves	26	243	208	61	500	6

Pollen analysis and biome reconstruction

Palynological analysis of the 40 samples from Och18-II-4 (see Supporting Information Table S1 for original data set) revealed 59 identified palynomorphs, including 15 AP taxa (i.e. trees, shrubs and dwarf shrubs), 33 NAP taxa (i.e. herbs, sedges and grasses), two aquatic plant taxa, five terrestrial cryptogam taxa (i.e. ferns and allies), and four taxa representing green algae colonies and other NPPs (i.e. *Botryococcus*, *Pediastrum*, *Glomus* and Chironomidae remains). In total, only 31 terrestrial pollen taxa exceed 0.5% [a universal threshold recommended by Prentice *et al.* (1996) for calculating biome scores], while others are below this level. Pollen concentration is moderately low throughout the record (Fig. 5A) and fluctuates around a mean value of 17 300 grains g^{-1}.

Visual inspection of the pollen diagram (Fig. 5A) demonstrates slight changes in the pollen taxon composition and percentages during the analysed core interval. The peak in Poaceae (ca. 51%) and the corresponding minimum in Cyperaceae (ca. 18%) percentages registered at a depth of about 645–640 cm is most noticeable. Quantitative CONISS analysis shows that the total sum of squares is <1.5 (Fig. 5B), which confirms close similarity between the pollen spectra.

The diagram (Fig. A) shows that NAP is predominant in the pollen assemblages throughout the Och18-II-4 record and varies between 82 and 97% (mean ca. 92.6%). The most abundant taxa are Poaceae (ca. 20–51%) and Cyperaceae (ca. 7–39%), followed by Brassicaceae (4.5–17.7%), Asteraceae subfamily Cichorioideae (4.6–15.8%), *Artemisia* (2–13%), Chenopodiaceae (1.8–3.6%), Asteraceae subfamily Asteroideae (1.8–3.5%) and other minor taxa. Boreal trees are represented by all major taxa, including *Betula* sect. *Albae* (0.6–4.8%), *Picea* (0.6–2.8%), *Pinus sibirica* type (up to 1.5%), *Pinus sylvestris* type (up to 2%), *Larix* (up to 0.6%) and *Abies* (up to 0.6%). *Betula* sect. *Nanae/Fruticosae* pollen (2–5.2%) and *Salix* (up to 3.2%) are the most representative boreal shrub taxa. Aquatics are minor pollen contributors as well as terrestrial cryptogams and their total sum never exceeds 0.7 and 1%, respectively. Among the identified NPPs, *Pediastrum*, *Botryococcus* and *Glomus* show continuous presence throughout the record (Fig. 5A).

The pollen-based biome reconstruction (Fig. 5C) shows highest scores for the steppe biome (16.5–23.6, ca. 20 on average) with a trend to lower values towards the top of the record. The tundra biome (11.3–16.6, ca. 14.5 on average) demonstrates lower scores than the steppe, but a trend to higher values towards the top. The taiga biome scores are relatively low and vary between 0.7 and 6.2 (2.7 on average).

Discussion

Lake history

The occurrence of freshwater ostracods in the investigated core section suggests the persistence of a lacustrine environment throughout the time interval analysed. The lowest analysed sample (656–655 cm) probably indicates a higher energy depositional environment, as suggested by the absence of juveniles and the presence of broken carapaces. In contrast, the presence of juveniles in the other five samples (all with *Cytherissa lacustris*) from the upper part of the Och18-II-4 section indicates a lower energy depositional environment with a low degree of post-mortem reworking of carapaces. *C. lacustris* is an endobenthic, Holarctic species that prefers oligo- to mesotrophic lakes, where it usually occurs in the profundal to sublittoral zone (Meisch, 2000). Although laboratory experiments show that *C. lacustris* may tolerate temperatures up to 24 °C for several weeks, field observations and ecological studies demonstrate that the species prefers water temperatures <18 °C (Newrkla, 1985; Danielopol *et al.*, 1988). The faunal shift, which occurred in the basal part of the Och18-II-4 section (between ca. 27 750 and 26 300 cal a BP), probably indicates a shift in habitat from a high-energy littoral zone to a relatively deeper sublittoral environment, pointing to an increase in water depth or/and distance from the coring site to the shoreline.

The sediment description reflects rather stable and uninterrupted sedimentation without strong changes for the entire core section. This is also reflected in the sedimentological and geochemical analyses that only show subtle changes between 657 and 500 cm. Grain-size changes to coarser particles occur only between 657 and 620 cm (coarser) and at 585 cm, pointing to possibly lowered lake levels.

Ti, K, Rb, Zr and Si indicate minerogenic input to the lake (Kylander *et al.*, 2011). Ti, K and Rb correlate strongly (Supporting Information Figs S1 and S2) and this is interpreted as reflecting detrital clay mineral input. The correlations between Si, Zr and Ti are less positive and suggest a combination of minerogenic (silicate minerals) and biogenic sources (Si as a component of diatom frustules). The biogenic SiO_2 values vary between 0.4 and 2.3%. As the catchment of Lake Ochaul exhibits Ca-bearing sediments (dolomite marls, anhydrite and gypsum within the Middle–Upper Cambrian Verkholenskaya suite) the origin of Ca may have allogenic (related to carbonate weathering in the catchment) and authigenic sources (Cohen, 2003). The strong correlation between Ca and Sr throughout the core section (Fig. S3) suggests that primarily authigenic calcite ($CaCO_3$) precipitation may be the main Ca source. This is corroborated by the negative correlation between Ca and the elements representing minerogenic input such as K, Rb and Ti (Pleskot *et al.*, 2018). Whereas the close correlation between P and Ca (Fig. S3) may point to mainly biogenically triggered authigenic calcite precipitation, there is no positive correlation between TOC and P. The reason for the latter probably is the rather low TOC content due to TOC decomposition under anoxic conditions. Higher Ca/Ti ratios together with the slightly coarser texture and less TOC possibly point to lake level lowering and unstable conditions during the period between ca. 26 920 and 25 830 cal a BP. Limnic conditions

prevailed throughout the record, as shown by the presence of ostracods and pyrite (FeS_2) in all analysed samples (Fig. 4). Iron sulphides are authigenic products of reductive diagenesis of magnetite (Fe_3O_4) or, most likely, greigite ($Fe^{2+}Fe^{3+}{}_2S_4$), which occurs in lacustrine sediments with clays and silts and is formed by magnetotactic and sulphate-reducing bacteria (Anthony *et al.*, 1990).

From the sedimentary proxies and the aforementioned interpretation, we distinguish the following four intervals (I–IV):

I. 657–620 cm (ca. 27 850–25 830 cal a BP): lowest TOC values and coarser detrital input may point to lower lake levels or a more littoral deposition in correspondence to the ostracod analysis that showed a higher energy depositional environment. By contrast, the relatively high and almost constantly increasing Ca/Ti ratios show that lacustrine calcite precipitation occurred. The decrease in mean grain sizes, interpreted as declining detrital input and a lower energy depositional environment, and recorded SiO_2bio fluctuations suggest rather unstable conditions and changes towards more stable, deeper environments during this phase.
II. 620–595 cm (ca. 25 830–24 460 cal a BP): highest concentrations of Chironomidae remains along with relative increase in SiO_2bio percentages, rising TOC values and low detrital input reflect a deeper lake and lowered calcite precipitation (low Ca/Ti ratios) and thus warmer conditions.
III. 595–560 cm (ca. 24 460–22 550 cal a BP): variations in increased Ca precipitation and thus also in the Ca/Ti ratios may point to a more fluctuating but slightly lower lake level with more detrital input (coarser grain-sizes), while the disappearance of Chironomidae remains and lower SiO_2bio percentages probably indicate colder conditions.
IV. 560–500 cm (ca. 22 550–20 400 cal a BP): this is the period with relatively high SiO_2bio values, lowest calcite production and constantly low Ca/Ti ratios without major changes. Also, the highest clay contents of the entire section point to stable conditions and a higher lake level.

Vegetation history

The analytical results obtained in this study allow discussion of the vegetation and environments around Lake Ochaul during the interval 27 850–20 400 cal a BP, with an average temporal resolution of approximately 180 years. The pollen diagram (Fig. 5A) demonstrates high percentages of herbaceous taxa in the pollen assemblage and indicates predominantly open vegetation in the area around Lake Ochaul. The pollen composition suggests that the vegetation cover contained grasses, sedges and diverse forb species, including *Artemisia* and other members of the aster family. The highest affinity scores calculated for the steppe and tundra biomes (Fig. 5C) support this qualitative interpretation of the pollen record and suggest that steppe and herbaceous tundra vegetation communities were widely spread in the study area under climate conditions substantially different from the present. This interpretation finds support in other published LGM pollen records that represent the vast area of Siberia (e.g. Edwards *et al.*, 2000; Prentice and Jolly, 2000; Binney *et al.*, 2017; Tarasov *et al.*, 2000, 2020). However, the record from Lake Ochaul presented here differs from the others in that it exhibits a noticeable (i.e. 1.4–9.2%, 3.7% on average) and constant presence of AP taxa (Fig. 7A), representing all dominant species of boreal trees (Fig. 5A) that grow in the region today (e.g. Belov *et al.*, 2002).

The AMS-dated pollen records of the KTK2 core (Bezrukova *et al.*, 2010) and the KTK10 core (Müller *et al.*, 2014) recovered from Lake Kotokel (Fig. 1B), located near the southern border of the modern taiga zone (Fig. 1C), ca. 200 km south-east of Lake Ochaul, also demonstrate the presence of boreal tree taxa in the LGM pollen assemblages (Fig. 7B), albeit in lower proportions than in Och18-II-4 (Fig. 7A). A similar picture (Fig. 7C) emerges when considering the LGM pollen record from Lake Billyakh (65°17′N, 126°47′E, 340 m a.s.l.; Müller *et al.*, 2010) located close to the northern limit of the boreal conifer forest zone, only 140 km south of the Arctic Circle and ca. 1650 km north-east of Lake Ochaul. These and some other robustly dated pollen and plant macrofossil records (e.g. Tarasov *et al.*, 2007; Williams *et al.*, 2011), representing the northern, central and southern part of the boreal forest zone of Eastern Siberia, also demonstrate the presence of tree pollen between ca. 28 000 and 20 000 cal a BP and support the hypothesis that small populations of boreal trees could survive the coldest interval of the last glacial in the refugia, both local (e.g. Bezrukova *et al.*, 2010; Müller *et al.*, 2010; Tarasov *et al.*, 2020) or/and located somewhere in Southern Siberia (e.g. Grichuk, 1984; Crowley, 1995; Petit *et al.*, 2008).

The cases in which AP in low numbers has been identified in LGM sediment samples from northern Eurasia (e.g. Lozhkin *et al.*, 2006; Bezrukova *et al.*, 2010; Müller *et al.*, 2010) are often explained by long-distance pollen transport and very sparse (i.e. desert-like) vegetation cover around the studied sites (e.g. Ray and Adams, 2001; Lozhkin *et al.*, 2006). The latter conclusion is based on lower-than-present pollen concentrations in the analysed sediment samples. In the Och18-II-4 record, the concentration of terrestrial pollen is moderately low and fluctuates around an average value of 17 300 grains g^{-1} (Fig. 5A). This is much lower than the values of 100 000–150 000 grains g^{-1} that were recorded in the Holocene samples from Lake Ochaul, between 8000 and 4000 cal a BP (Kobe *et al.*, 2020), but comparable to the pollen concentration recorded by Müller *et al.* (2010) in the modern surface sample from Lake Billyakh [i.e. 15 300 grains g^{-1}, situated in the larch-dominated forest zone of northern Yakutia (Fig. 1A)], and higher than in the Late Holocene sediment samples from Lake Lama (i.e. < 10 000 grains g^{-1}) located at an altitude of 53 m a.s.l. at the western margin of the Putorana Plateau (Fig. 1A) and surrounded by taiga forest with spruce, larch and birch (Andreev *et al.*, 2004). None of the analysed LGM pollen spectra from Lake Ochaul (Fig. 5A) recemble modern surface pollen spectra collected from an arctic desert or barren environment (Tarasov *et al.*, 2007). The biome reconstruction approach applied to the reference pollen data set from Eastern Siberia showed very good agreement between actual vegetation (i.e. tundra, cold deciduous and taiga forest) and reconstructed biomes, suggesting that long-distance AP transport does not influence results of pollen-based vegetation reconstruction (Müller *et al.*, 2010).

Absence of radiocarbon-dated woody plant macrofossils in the sedimentary records from Siberia assigned to the LGM interval was commonly taken as proof of year-round extremely cold and dry environments similar to that of arctic desert or arctic herbaceous tundra (see Kageyama *et al.*, 2001; Kaplan *et al.*, 2003; MacDonald *et al.*, 2000, 2008; Tarasov *et al.*, 2020 for detailed discussion and references).

The existing palaeontological and archaeological data from Siberia (Tarasov *et al.*, 2020) cannot be explained by a 'year-round colder-than-present climate scenario'. Although the $\delta^{18}O$ data from Greenland ice cores (Fig. 7G), commonly considered as a high-resolution record of Northern Hemisphere temperature (e.g. Seierstad *et al.*, 2014), indicate substantially lower-than-present mean annual temperature

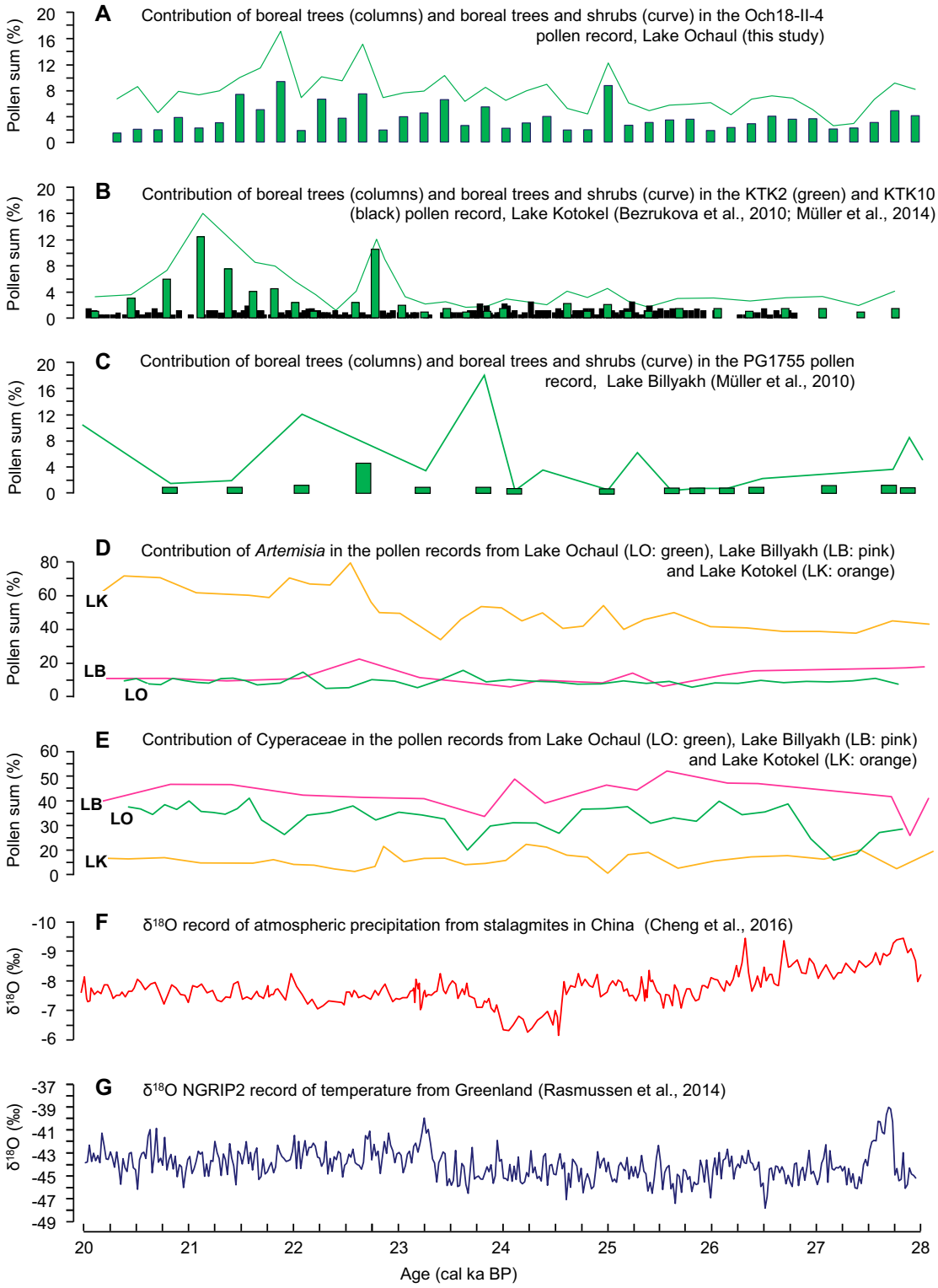

Figure 7. Summary chart showing (A–E) selected results derived from the Last Glacial Maximum pollen records of Lake Ochaul (this study), Lake Kotokel (Bezrukova *et al.*, 2010; Müller *et al.*, 2014) and Lake Billyakh (Müller *et al.*, 2010), representing central, southern and northern parts of Eastern Siberia, along with selected records of Northern Hemisphere climate showing (F) the $\delta^{18}O$ record of precipitation from Chinese stalagmites (Cheng *et al.*, 2016) and (G) the $\delta^{18}O$ ice core record from Greenland (Rasmussen *et al.*, 2014; Seierstad *et al.*, 2014), as an indicator of mean air temperature. Each record is plotted against its original chronology, as published in the respective publication. [Color figure can be viewed at wileyonlinelibrary.com].

during the LGM, they do not tell how these changes influenced the summer and winter seasons in the different regions of Eurasia. Indeed, Zech *et al.* (2010), using alkane biomarker and pollen records from a ca. 240-ka-old loess–palaeosol sequence from the Tumara site in the south-western foreland of the Verkhoyansk Mountains, north-east Siberia (63°36′N, 129°58′E; 120 m a.s.l.), argued that it was not mainly temperature changes, but rather increasing aridity and continentality during the course of the last glacial that favoured the expansion of herbaceous vegetation (i.e. 'mammoth steppe'). Relatively warm LGM summers with mean July temperatures above 12 °C were reconstructed using an indicator-species approach applied to an accurately dated plant macrofossil record from the Bykovsky Peninsula at the

Laptev Sea coast (Kienast *et al.*, 2005) and a chironomid-based reconstruction from Lake Kotokel (Tarasov *et al.*, 2019). Both studies suggest a ca. 3.5 °C higher than present summer temperature for the southern part of Eastern Siberia between ca. 24 000 and 22 000 cal a BP. These reconstructions and other recently published data from Siberia (e.g. Ashastina *et al.*, 2018) indicate an extremely continental, relatively dry climate with winters colder and summers distinctly warmer than at present in the eastern Siberian Arctic during the LGM and contradict the 'cold summer scenario' with mean August temperatures ca. 6–8 °C lower than present across most of Siberia (e.g. Frenzel *et al.*, 1992; Ray and Adams, 2001; Strandberg *et al.*, 2011).

Much more consistent are results of proxy-based reconstructions and climate model simulations of atmospheric precipitation and water budget in the eastern part of Eurasia during the LGM (e.g. Frenzel *et al.*, 1992; Kienast *et al.*, 2005; Yanase and Abe-Ouchi, 2007; Andreev *et al.*, 2011; Strandberg *et al.*, 2011). All cited publications demonstrate a year-round decrease in precipitation leading to a thin snow cover and spread of herbaceous plants to the disadvantage of boreal trees and shrubs (e.g. Prentice and Jolly, 2000; Kaplan *et al.*, 2003; Tarasov *et al.*, 2020). The main differences are in absolute values of reconstructed or simulated variables, but not in the general trend towards a drier-than-present LGM climate. Thus, the pollen-based reconstruction (Tarasov *et al.*, 2013b) derived from the LGM record of Lake Billyakh (Müller *et al.*, 2010) demonstrates a 25% decrease in annual precipitation compared to the modern average of ca. 350 mm. The reconstruction derived from the LGM pollen record of Lake Kotokel (Bezrukova *et al.*, 2010) shows an even more pronounced, i.e. ca. 45%, decrease in atmospheric precipitation during the LGM in the southern part of eastern Siberia (Tarasov *et al.*, 2017). Although qualitative interpretations and quantitative reconstructions derived from various proxies consistently indicate a drier-than-present LGM climate (e.g. Fig. 7F; Cheng *et al.*, 2016) and open, predominantly mosaic vegetation (e.g. Andreev *et al.*, 2003; Kienast *et al.*, 2005; Ashastina *et al.*, 2018) in the Asian high latitudes between Lake Gerditzy (Fig. 1A) in the Polar Urals (Svendsen *et al.*, 2014) and Lake El'gygytgyn (Fig. 1A) on the Chukotka Peninsula (Lozhkin *et al.*, 2006), the published lake and vegetation records (e.g. Tarasov *et al.*, 2020) do not support extreme aridity and a desert-like or ice-covered landscape as suggested in some of the earlier reconstructions (e.g. Ray and Adams, 2001). Moreover, evidence that boreal trees did not disappear from the vegetation cover during the LGM comes from radiocarbon-dated archaeological wood and charcoal pieces collected in the middle latitudes of Siberia and the Russian Far East (Fig. 1A; Vasil'ev *et al.*, 2002). The long pollen record from the Khoe site (Fig. 1A) in the central part of Sakhalin Island reveals high percentages of pine, larch and spruce pollen between 30 and 15 cal ka BP, suggesting that boreal trees still occupied up to 30–40% of the landscape (Leipe *et al.*, 2015).

Here, we use selected results derived from the LGM parts of the Lake Billyakh (Müller *et al.*, 2010), Lake Ochaul (this study) and Lake Kotokel (Bezrukova *et al.*, 2010; Müller *et al.*, 2014) pollen records (Fig. 7A–E), representing the northern, central and southern part of the modern boreal forest zone in Eastern Siberia, to discuss this issue.

As shown in the original publications and in Fig. 5 of this study, none of the three records indicates extreme aridity, but continuous lacustrine sedimentation, virtual absence of desert indicator taxa and very low percentages of Chenopodiaceae pollen commonly associated with desert and/or barren environments. Therefore, a contribution of *Artemisia* pollen is the most common and reliable indicator of steppe vegetation and climate aridity in Eurasia (Prentice *et al.*, 1996; Tarasov *et al.*, 1998a). The southernmost record of Lake Kotokel shows the highest percentages of *Artemisia* pollen (40–80%, ca. 60% on average), while its contribution in Lake Billyakh does not exceed 20% and in Lake Ochaul 15% of the total pollen sum (Fig. 7D). These data indicate a steep moisture gradient between areas south and north of Lake Baikal and suggest that the area around Lake Ochaul represents the least dry environment of the three representative sites. This conclusion is supported by the highest and continuous contribution of boreal tree and shrub pollen to the Ochaul record (Fig. 7A).

In the biome–taxon matrix suggested for the pollen-based vegetation reconstruction in northern Eurasia (Prentice *et al.*, 1996; Tarasov *et al.*, 1998a, b), Cyperaceae represents the tundra biome and therefore can be regarded as a zonal indicator of colder environments. The northernmost record of Lake Billyakh shows highest percentages of Cyperaceae pollen (40–50% on average), moderately high percentages are recorded in the Lake Ochaul (ca. 30% on average) and the lowest of all (ca. 10% on average) in the Lake Kotokel record (Fig. 7E). These data primarily reflect the temperature gradient across Eastern Siberia, indicating coldest conditions in the north and warmest in the south. The selected pollen records (Fig. 7A–E) indicate that this part of Eastern Siberia, including the Upper Lena region, was one of the areas that served as a refugium for boreal trees during the LGM. We argue that pollen of boreal trees in the Ochaul record probably represents local tree populations and not pollen transported from far-distant regions in the south. In the latter case, the AP content in the LGM spectra from Lake Kotokel would be more significant than it currently is (Fig. 7B).

Directly dated evidence of LGM woody plants from the study region is still rare. Results of microcharcoal analysis at the archaeological sites Kovrizhka III and IV (Fig. 1A) in the lower Vitim River valley (Baikal–Patom Highlands) north-east of Lake Baikal (57°49′N, 113°55′E) reveal growth of trees and shrubs there during the LGM (Henry *et al.*, 2018). The modern vegetation composition of the valley resembles that of Lake Ochaul. Forests are dominated by larch (*Larix gmelinii*) and birch (*Betula platyphylla*) with less frequent occurrence of spruce (*Picea obovata*), pines (*Pinus sibirica* and *Pinus sylvestris*) and fir (*Abies sibirica*), and abundant birch and willow shrubs occupying swampy floodplain areas. The charcoal assemblage AMS-dated to ca. 19 250–18 350 cal a BP reveals remains of *Salix*, *Larix*/*Picea*, *Betula*, *Juniperus* and undetermined conifers (Henry *et al.*, 2018), suggesting that Upper Palaeolithic hunter-gatherers collected wood for their fires.

Conclusions

Published pollen and plant macrofossil records from the northern and southern part of the taiga zone in Siberia demonstrate that boreal forests – the most characteristic feature of Eurasian vegetation – quickly established there during the Lateglacial and early Holocene interval, suggesting that small tree populations could have survived the generally colder- and drier-than-present glacial period somewhere in the region. However, due to a lack of high-resolution pollen and radiocarbon-dated macrofossil data from the vast central regions of Eastern Siberia, there is no agreement on if and where boreal trees could have survived during the LGM. The current study presents a sedimentary record from Lake Ochaul in the Upper Lena region and contributes to a better understanding of the complex spatial vegetation pattern across Siberia ca. 28 000–20 000 cal a BP. Together with existing modern and fossil pollen data from the wider study region, the current record provides further evidence for the long-debated presence of boreal trees and shrubs and the dominance of productive herbaceous vegetation in Eastern Siberia throughout the LGM. Our results show that the Upper Lena was another region in which refugia for arboreal taxa existed and that

far-distant pollen transport can be ruled out as the source of the detected AP. Comparison of the *Artemisia* and Cyperaceae records from different sites in Eastern Siberia allows us to reconstruct gradients in available moisture and temperature, respectively. During the LGM, regions south/south-east of Lake Baikal were warmer and drier than those in the north/north-west (including Cis-Baikal), which provides an explanation for the absence of trees in the Trans-Baikal region. Our study emphasizes that moisture availability rather than thermal conditions probably played a decisive role for tree and shrub growth during the coldest stage of the last glacial.

Supporting information

Additional supporting information may be found in the online version of this article at the publisher's web-site.

Acknowledgements. The research presented here was financially supported via research grants from the Russian Foundation for Basic Research (RFBR No. 19-05-00328 and No. 20-05-00247), the German Research Foundation (DFG TA 540/5, MU 3181/1), the Vinogradov Institute of Geochemistry, Siberian Branch of the Russian Academy of Sciences (project No. 0350-2017-0026), the Russian Science Foundation (project No. 19-17-00216, geomorphology), the Government of The Russian Federation (project No. 075-15-2019-866), Siberian Branch of the Russian Academy of Sciences (Integration Project No. 0341-2017-0001) and by the Baikal Archaeology Project (BAP: https://baikalproject.artsrn.ualberta.ca/). The doctoral stipend of F. Kobe at the Freie Universität Berlin (FU Berlin) is financed via a grant from the Social Sciences and Humanities Research Council of Canada for the project 'Individual life histories in long-term culture change: Holocene hunter-gatherers in Northern Eurasia' (SSHRC Partnership grant No. 895-2018-1004). The work of J. Gliwa contributes to the research project 'Ground Check in Northeast Asia' of the German Archaeological Institute (DAI). The authors' special thanks go to I. A. Filinov, I. O. Nechaev and M. A. Krainov (Institute of Geochemistry, Irkutsk) for their valuable assistance in organizing field work and drilling Lake Ochaul, and to A. Janus (DAI) and A. Görnt (FU Berlin) for assistance in the laboratory and SEM work. We also thank two anonymous reviewers for their valuable comments and suggestions. Open Access funding enabled and organized by Projekt DEAL.

Data availability statement

All data generated or analysed during this study are included in this published article.

Abbreviations. AMS, accelerator mass spectrometry; cps, counts per second; Indet, indetermined; LBR, Lake Baikal Region; LGM, Last Glacial Maximum; P-ED XRF, portable energy-dispersive X-ray fluorescence spectrometry; rpm, rotations per minute; TC, total carbon; TIC, total inorganic carbon; TOC, total organic carbon; XRD, X-ray diffraction; aDNA, ancient DNA; AP, arboreal pollen; BAP, Baikal Archaeology Project; ICP-OES, inductively coupled plasma optical emission spectrometry; NAP, non-arboreal pollen; NPP, non-pollen palynomorph; SEM, scanning electron microscopy; SPT, sodium polytungstate; SRTM, shuttle radar topography mission; TN, total nitrogen.

References

Allen JRL, Thornley DM. 2004. Laser granulometry of Holocene estuarine silts: effects of hydrogen peroxide treatment. *The Holocene* **14**: 290–295. https://doi.org/10.1191/0959683604hl681rr

Alpat'ev AM, Arkhangel'skii AM, Podoplelov NY *et al.* 1976. Fizicheskaya geografiya SSSR [Aziatskaya chast]. Vysshaya Shkola: Moscow (in Russian).

Andreev AA, Schirrmeister L, Tarasov PE *et al.* 2011. Vegetation and climate history in the Laptev Sea region (Arctic Siberia) during Late Quaternary inferred from pollen records. *Quaternary Science Reviews* **30**: 2182–2199. https://doi.org/10.1016/j.quascirev.2010.12.026

Andreev AA, Tarasov PE, Klimanov VA *et al.* 2004. Vegetation and climate changes around the Lama Lake, Taymyr Peninsula, Russia during the Late Pleistocene and Holocene. *Quaternary International* **122**: 69–84. https://doi.org/10.1016/j.quaint.2004.01.032

Andreev AA, Tarasov PE, Siegert C *et al.* 2003. Late Pleistocene and Holocene vegetation and climate on the northern Taymyr Peninsula, Arctic Russia. *Boreas* **32**: 484–505. https://doi.org/10.1080/03009480310003388

Anthony JW, Bideaux RA, Bladh KW *et al.* 1990. Handbook of Mineralogy I (Elements, Sulfides, Sulfosalts). Mineralogical Society of America: Chantilly.

Ashastina K, Kuzmina S, Rudaya N *et al.* 2018. Woodlands and steppes: Pleistocene vegetation in Yakutia's most continental part recorded in the Batagay permafrost sequence. *Quaternary Science Reviews* **196**: 38–61. https://doi.org/10.1016/j.quascirev.2018.07.032

Belov AV, Ljamkin VF, Sokolova LP. 2002. Cartographic study of biota. Oblmashinform: Irkutsk (in Russian).

Beug H-J. 2004. Leitfaden der Pollenbestimmung: Für Mitteleuropa und Angrenzende Gebiete. Pfeil: München.

Bezrukova EV, Tarasov PE, Solovieva N *et al.* 2010. Last glacial-interglacial vegetation and environmental dynamics in southern Siberia: chronology, forcing and feedbacks. *Palaeogeography, Palaeoclimatology, Palaeoecology* **296**: 185–198. https://doi.org/10.1016/j.palaeo.2010.07.020

Binney H, Edwards M, Macias-Fauria M *et al.* 2017. Vegetation of Eurasia from the last glacial maximum to present: key biogeographic patterns. *Quaternary Science Reviews* **157**: 80–97. https://doi.org/10.1016/j.quascirev.2016.11.022

Binney HA, Willis KJ, Edwards ME *et al.* 2009. The distribution of late-Quaternary woody taxa in northern Eurasia: evidence from a new macrofossil database. *Quaternary Science Reviews* **28**: 2445–2464. https://doi.org/10.1016/j.quascirev.2009.04.016

Boyarkin VM. 2007. Geografiya Irkutskoi Oblasti. Publishing House: Sarma (in Russian).

Bronk Ramsey C. 1995. Radiocarbon calibration and analysis of stratigraphy: the OxCal program. *Radiocarbon* **37**: 425–430. https://doi.org/10.1017/S0033822200030903

Bronstein ZS. 1947. Ostracoda presnykh vod. Fauna SSSR. Rakoobraznye. Tom II: Vypusk1. Izdatel'stvo Akedemii Nauk SSR: Moscow (in Russian).

Brubaker LB, Anderson PM, Edwards ME *et al.* 2005. Beringia as a glacial refugium for boreal trees and shrubs: new perspectives from mapped pollen data. *Journal of Biogeography* **32**: 833–848. https://doi.org/10.1111/j.1365-2699.2004.01203.x

Cheng H, Edwards RL, Sinha A *et al.* 2016. The Asian monsoon over the past 640,000 years and ice age terminations. *Nature* **534**: 640–646. https://doi.org/10.1038/nature18591

Clark PU, Dyke AS, Shakun JD *et al.* 2009. The Last Glacial maximum. *Science* **325**: 710–714. https://doi.org/10.1126/science.1172873

Cohen AS. 2003. *Paleolimnology: the History and Evolution of Lake Systems*. Oxford University Press: Oxford.

Crowley TJ. 1995. Ice age terrestrial carbon changes revisited. *Global Biogeochemical Cycles* **9**: 377–389. https://doi.org/10.1029/95GB01107

Danielopol DL, Geiger W, Töui-Derbr-Farmer M *et al.* 1988. In Search of Cypris and Cythere—A Report of the Evolutionary Ecological Project on Linmic Ostracoda from the Mondsee (Austria). In Proceedings of the Ninth International Symposium on Ostracoda. Developments in Palaeontology and Stratigraphy, Hanai T, Ikeya N, Ishizaki K (eds). Elsevier: Amsterdam; 485–500.

DeFries RS, Hansen MC, Townshend JRG. 2000. Global continuous fields of vegetation characteristics: a linear mixture model applied to multi-year 8 km AVHRR data. *International Journal of Remote Sensing* **21**: 1389–1414. https://doi.org/10.1080/014311600210236

Demske D, Heumann G, Granoszewski W *et al.* 2005. Late glacial and Holocene vegetation and regional climate variability evidenced in high-resolution pollen records from Lake Baikal. *Global and Planetary Change* **46**: 255–279. https://doi.org/10.1016/j.gloplacha.2004.09.020

Demske D, Tarasov PE, Nakagawa T *et al.* 2013. Atlas of pollen, spores and further non-pollen palynomorphs recorded in the

glacial-interglacial late Quaternary sediments of Lake Suigetsu, Central Japan. *Quaternary International* **290–291**: 164–238.

DIN EN. 2001. *Charakterisierung von Schlämmen – Bestimmung von Spurenelementen und Phosphor – Extraktionsverfahren mit Königswasser; Deutsche Fassung*. Beuth Verlag: Berlin.

Edwards ME, Anderson PM, Brubaker LB *et al*. 2000. Pollen-based biomes for Beringia 18,000, 6000 and 0 14C yr bp. *Journal of Biogeography* **27**: 521–554. https://doi.org/10.1046/j.1365-2699.2000.00426.x

Fiedel SJ, Kuzmin YV. 2007. Radiocarbon date frequency as an index of intensity of Paleolithic occupation of Siberia: did humans react predictably to climate oscillations? *Radiocarbon* **49**: 741–756. https://doi.org/10.1017/S0033822200042624

Frenzel B, Pecsi B, Velichko AA. 1992. Atlas of palaeoclimates and palaeoenvironments of the northern hemisphere INQUA/Hungarian Academy of Sciences: Budapest.

Galaziy GI. 1993. Baikal Atlas. Federalnaya sluzhba geodezii i kartografii Rossii: Moscow (in Russian).

Grichuk V. 1984. Late Pleistocene vegetation history. In *Late Quaternary Environments of the Soviet Union*, Velichko AA (ed). University of Minnesota Press: Minneapolis; 155–178.

Grimm EC. 1987. Coniss: a Fortran 77 program for stratigraphically constrained cluster analysis by the method of incremental sum of squares. *Computers and Geosciences* **13**: 13–35. https://doi.org/10.1016/0098-3004(87)90022-7

Grimm EC. 2011. Tilia 1.7.16 Software. Illinois State Museum, Research and Collection Center: Springfield.

Guiot J, Goeury C. 1996. PPPBASE, a software for statistical analysis of palaeoecological and palaeoclimatological data. *Dendrochronologia* **14**: 295–300.

Hansen MC, Potapov PV, Moore R *et al*. 2013. High-resolution global maps of 21st-century forest cover change. *Science* **342**: 850–853. https://doi.org/10.1126/science.1244693. [PubMed: 24233722].

Henry A, Bezrukova EV, Teten'kin AV *et al*. 2018. New data on vegetation and climate reconstruction in the Baikal-Patom Highland (Eastern Siberia) in the Last Glacial Maximum and Early Holocene. *Doklady Earth Sciences* **478**: 241–244. https://doi.org/10.1134/S1028334X18020113

Jarvis A, Reuter HI, Nelson A *et al*. 2008. Hole-filled Seamless SRTM Data V4. International Centre for Tropical Agriculture (CIAT).

Kageyama M, Peyron O, Pinot S *et al*. 2001. The Last Glacial Maximum climate over Europe and western Siberia: a PMIP comparison between models and data. *Climate Dynamics* **17**: 23–43. https://doi.org/10.1007/s003820000095

Kaplan JO, Bigelow NH, Prentice IC. 2003. Climate change and Arctic ecosystems: 2. Modeling, paleodata-model comparisons, and future projections. *Journal of Geophysical Research* **108**: 8171. https://doi.org/10.1029/2002JD002559

Kaplan JO, Pfeiffer M, Kolen JCA *et al*. 2016. Large scale Anthropogenic reduction of forest cover in last glacial maximum Europe. *PLoS ONE* **11**: e0166726. https://doi.org/10.1371/journal.pone.0166726

Kienast F, Schirrmeister L, Siegert C *et al*. 2005. Palaeobotanical evidence for warm summers in the East Siberian Arctic during the last cold stage. *Quaternary Research* **63**: 283–300. https://doi.org/10.1016/j.yqres.2005.01.003

Kobe F, Bezrukova EV, Leipe C *et al*. 2020. Holocene vegetation and climate history in Baikal Siberia reconstructed from pollen records and its implications for archaeology. Archaeological Research in Asia 23 [https://doi.org/10.1016/j.ara.2020.100209]

Kylander ME, Ampel L, Wohlfarth B *et al*. 2011. High-resolution X-ray fluorescence core scanning analysis of Les Echets (France) sedimentary sequence: new insights from chemical proxies. *Journal of Quaternary Science* **26**: 109–117. https://doi.org/10.1002/jqs.1438

Lambeck K, Rouby H, Purcell A *et al*. 2014. Sea level and global ice volumes from the last glacial maximum to the Holocene. *Proceedings of the National Academy of Sciences of the United States of America* **111**: 15296–15303. https://doi.org/10.1073/pnas.1411762111

Leipe C, Kobe F, Müller S. 2019. Testing the performance of sodium polytungstate and lithium heteropolytungstate as non-toxic dense media for pollen extraction from lake and peat sediment samples. *Quaternary International* **516**: 207–214. https://doi.org/10.1016/j.quaint.2018.01.029

Leipe C, Nakagawa T, Gotanda K *et al*. 2015. Late Quaternary vegetation and climate dynamics at the northern limit of the East Asian summer monsoon and its regional and global-scale controls. *Quaternary Science Reviews* **116**: 57–71. https://doi.org/10.1016/j.quascirev.2015.03.012

Lozhkin AV, Anderson PM, Matrosova TV *et al*. 2006. The pollen record from El'gygytgyn Lake: implications for vegetation and climate histories of northern Chukotka since the late Middle Pleistocene. *Journal of Paleolimnology* **37**: 135–153. https://doi.org/10.1007/s10933-006-9018-5

MacDonald GM, Kremenetski KV, Beilman DW. 2008. Climate change and the northern Russian treeline zone. *Philosophical Transactions of the Royal Society of London. Series B, Biological Sciences* **363**: 2285–2299. https://doi.org/10.1098/rstb.2007.2200

MacDonald GM, Velichko AA, Kremenetski CV *et al*. 2000. Holocene treeline history and climate change across northern Eurasia. *Quaternary Research* **53**: 302–311. https://doi.org/10.1006/qres.1999.2123

Mäkelä EM. 1996. Size distinctions between Betula pollen types – a review. *Grana* **35**: 248–256. https://doi.org/10.1080/00173139609430011

Mazepova GF. 1990. Rakushkovye Rachki (Ostracoda) Baykala. Izdatel'stvo Akademii Nauk SSSR, Sibirskoe Otdelenie, Limnologicheskii Institut: Irkutsk (in Russian).

Meisch C. 2000. Freshwater Ostracoda of Western and Central Europe. Spektrum Akademischer Verlag: Heidelberg.

Melles M, Brigham-Grette J, Minyuk PS *et al*. 2012. 2.8 million years of Arctic climate change from Lake El'gygytgyn, NE Russia. *Science* **337**: 315–320. https://doi.org/10.1126/science.1222135

Mikutta R, Kleber M, Kaiser K *et al*. 2005. Review: organic matter removal from soils using hydrogen peroxide, sodium hypochlorite, and disodium peroxodisulfate. *Soil Science Society of America Journal* **69**: 120–135. https://doi.org/10.2136/sssaj2005.0120

Mortlock RA, Froelich PN. 1989. A simple method for the rapid determination of biogenic opal in pelagic marine sediments. *Deep Sea Research Part A. Oceanographic Research* **Papers 36**: 1415–1426. https://doi.org/10.1016/0198-0149(89)90092-7

Müller S, Tarasov PE, Andreev AA *et al*. 2010. Late Quaternary vegetation and environments in the Verkhoyansk Mountains region (NE Asia) reconstructed from a 50-kyr fossil pollen record from Lake Billyakh. *Quaternary Science Reviews* **29**: 2071–2086. https://doi.org/10.1016/j.quascirev.2010.04.024

Müller S, Tarasov PE, Hoelzmann P *et al*. 2014. Stable vegetation and environmental conditions during the Last Glacial Maximum: new results from Lake Kotokel (Lake Baikal region, southern Siberia, Russia). *Quaternary International* **348**: 14–24. https://doi.org/10.1016/j.quaint.2013.12.012

Nakagawa T. 2007. Double-L channel: an amazingly non-destructive method of continuous sub-sampling from sediment cores. *Quaternary International* **167–168**(Suppl): 298.

Nakagawa T, Edouard J-L, de Beaulieu J-L. 2000. A scanning electron microscopy (SEM) study of sediments from Lake Cristol, southern French Alps, with special reference to the identification of Pinus cembra and other Alpine Pinus species based on SEM pollen morphology. *Review of Palaeobotany and Palynology* **108**: 1–15. https://doi.org/10.1016/S0034-6667(99)00030-5

Newrkla P. 1985. Respiration of Cytherissa lacustris (Ostracoda) at different temperatures and its tolerance towards temperature and oxygen concentration. *Oecologia* **67**: 250–254. https://doi.org/10.1007/BF00384294

Petit RJ, Hu FS, Dick CW. 2008. Forests of the past: A window to future changes. *Science* **320**: 1450–1452. https://doi.org/10.1126/science.1155457. [PubMed: 18556547].

Pleskot K, Tjallingii R, Makohonienko M *et al*. 2018. Holocene paleohydrological reconstruction of Lake Strzeszyńskie (western Poland) and its implications for the central European climatic transition zone. *Journal of Paleolimnology* **59**: 443–459. https://doi.org/10.1007/s10933-017-9999-2

Prentice C, Guiot J, Huntley B *et al*. 1996. Reconstructing biomes from palaeoecological data: a general method and its application to

European pollen data at 0 and 6 ka. *Climate Dynamics* **12**: 185–194. https://doi.org/10.1007/BF00211617

Prentice IC, Cramer W, Harrison SP *et al*. 1992. Special paper: a global biome model based on plant physiology and dominance, soil properties and climate. *Journal of Biogeography* **19**: 117–134. https://doi.org/10.2307/2845499

Prentice IC, Jolly D, Biome 6000 Participants. 2000. Mid-Holocene and glacial-maximum vegetation geography of the northern continents and Africa. *Journal of Biogeography* **27**: 507–519. https://doi.org/10.1046/j.1365-2699.2000.00425.x

Prokopenko AA, Bezrukova EV, Khursevich GK *et al*. 2010. Climate in continental interior Asia during the longest interglacial of the past 500 000 years: the new MIS 11 records from Lake Baikal, SE Siberia. *Climate of the Past* **6**: 31–48. https://doi.org/10.5194/cp-6-31-2010

Rasmussen SO, Bigler M, Blockley SP *et al*. 2014. A stratigraphic framework for abrupt climatic changes during the Last Glacial period based on three synchronized Greenland ice-core records: refining and extending the INTIMATE event stratigraphy. *Quaternary Science Reviews* **106**: 14–28. https://doi.org/10.1016/j.quascirev.2014.09.007

Ray N, Adams JM. 2001. A GIS-based vegetation map of the World at the last glacial maximum (25,000–15,000 BP). *Internet Archaeology* **11**. https://doi.org/10.11141/ia.11.2

Reille M. 1992. *Pollen et Spores d'Europe et d'Afrique du Nord. Laboratoire de Botanique Historique et Palynologie*. URA CNRS: Marseille.

Reille M. 1995. Pollen et Spores d'Europe et d' Afrique du Nord. Supplement 1. Laboratoire de Botanique Hislorique el Palynologie. URA CNRS: Marseille.

Reille M. 1998. Pollen et Spores d'Europe et d' Afrique du Nord. Supplement 2. Laboratoire de Botanique Hislorique el Palynologie. URA CNRS: Marseille.

Reimer PJ, Austin WEN, Bard E *et al*. 2020. The IntCal20 Northern Hemisphere radiocarbon age calibration curve (0–55 cal kBP). *Radiocarbon* **62**: 725–757. https://doi.org/10.1017/RDC.2020.41

Savelieva LA, Raschke EA, Titova DV. 2013. Photographic atlas of plants and pollen of the Lena River Delta. St Petersburg State University: St Petersburg.

Seierstad IK, Abbott PM, Bigler M *et al*. 2014. Consistently dated records from the Greenland GRIP, GISP2 and NGRIP ice cores for the past 104 ka reveal regional millennial-scale δ18O gradients with possible Heinrich event imprint. *Quaternary Science Reviews* **106**: 29–46. https://doi.org/10.1016/j.quascirev.2014.10.032

Shao Y, Anhäuser A, Ludwig P *et al*. 2018. Statistical reconstruction of global vegetation for the last glacial maximum. *Global and Planetary Change* **168**: 67–77. https://doi.org/10.1016/j.gloplacha.2018.06.002

Shumilova LV. 1960. The main features of the natural vegetation cover of Siberia and its geographical distribution. In Proceedings of the Tomsk State University 148; 171–182 (in Russian).

Stockmarr J. 1971. Tablets with spores used in absolute pollen analysis. *Pollen et Spores* **13**: 614–621.

Strandberg G, Brandefelt J, Kjellström E *et al*. 2011. High-resolution regional simulation of last glacial maximum climate in Europe. *Tallus* **63a**: 107–125.

Sun D, Bloemendal J, Rea DK *et al*. 2002. Grain-size distribution function of polymodal sediments in hydraulic and aeolian environments, and numerical partitioning of the sedimentary components. *Sedimentary Geology* **152**: 263–277. https://doi.org/10.1016/S0037-0738(02)00082-9

Svendsen JI, Krüger LC, Mangerud J *et al*. 2014. Glacial and vegetation history of the Polar Ural Mountains in northern Russia during the last ice age, marine isotope stages 5–2. *Quaternary Science Reviews* **92**: 409–428. https://doi.org/10.1016/j.quascirev.2013.10.008

Tarasov PE, Andreev AA, Anderson PM *et al*. 2013a. A pollen-based biome reconstruction over the last 3.562 million years in the Far East Russian Arctic – new insights into climate–vegetation relationships at the regional scale. *Climate of the Past* **9**: 2759–2775. https://doi.org/10.5194/cp-9-2759-2013

Tarasov PE, Bezrukova E, Karabanov E *et al*. 2007. Vegetation and climate dynamics during the Holocene and Eemian interglacials derived from Lake Baikal pollen records. *Palaeogeography, Palaeoclimatology, Palaeoecology* **252**: 440–457. https://doi.org/10.1016/j.palaeo.2007.05.002

Tarasov PE, Bezrukova EV, Müller S *et al*. 2017. Climate and vegetation history. In Holocene Zooarchaeology of Cis-Baikal, Losey RJ, Nomokonova T (eds). Nünnerich–Asmus Verlag & Media GmbH: Mainz; 15–26.

Tarasov PE, Cheddadi R, Guiot J *et al*. 1998a. A method to determine warm and cool steppe biomes from pollen data; application to the Mediterranean and Kazakhstan Regions. *Journal of Quaternary Science* **13**: 335–344. https://doi.org/10.1002/(SICI)1099-1417(199807/08)13:4%3C335::AID-JQS375%3E3.0.CO;2-A

Tarasov PE, Granoszewski W, Bezrukova E *et al*. 2005. Quantitative reconstruction of the last interglacial vegetation and climate based on the pollen record from Lake Baikal, Russia. *Climate Dynamics* **25**: 625–637. https://doi.org/10.1007/s00382-005-0045-0

Tarasov PE, Ilyashuk BP, Leipe C *et al*. 2019. Insight into the Last Glacial Maximum climate and environments of the Baikal region. *Boreas* **48**: 488–506. https://doi.org/10.1111/bor.12330

Tarasov PE, Leipe C, Wagner M. 2020. Environments during the spread of anatomically modern humans across northern Asia 50–10 cal kyr BP: what do we know and what would we like to know? Quaternary International [https://doi.org/10.1016/j.quaint.2020.10.030]

Tarasov PE, Müller S, Andreev A *et al*. 2009. Younger Dryas Larix in eastern Siberia: a migrant or survivor? *PAGES News* **17**: 122–123. https://doi.org/10.22498/pages.17.3.122

Tarasov PE, Müller S, Zech M *et al*. 2013b. Last glacial vegetation reconstructions in the extreme-continental eastern Asia: potentials of pollen and n-alkane biomarker analyses. *Quaternary International* **290–291**: 253–263. https://doi.org/10.1016/j.quaint.2012.04.007

Tarasov PE, Volkova VS, Webb T III *et al*. 2000. Last Glacial Maximum biomes reconstructed from pollen and plant macrofossil data from northern Eurasia. *Journal of Biogeography* **27**: 609–620. https://doi.org/10.1046/j.1365-2699.2000.00429.x

Tarasov PE, Webb T III, III, Andreev AA *et al*. 1998b. Present-day and mid-Holocene biomes reconstructed from pollen and plant macrofossil data from the former Soviet Union and Mongolia. *Journal of Biogeography* **25**: 1029–1053. https://doi.org/10.1046/j.1365-2699.1998.00236.x

Tautenhahn S, Lichstein JW, Jung M *et al*. 2016. Dispersal limitation drives successional pathways in Central Siberian forests under current and intensified fire regimes. *Global Change Biology* **22**: 2178–2197. https://doi.org/10.1111/gcb.13181

van Geel B. 1978. A palaeoecological study of Holocene peat bog sections in Germany and the Netherlands, based on the analysis of pollen, spores and macro- and microscopic remains of fungi, algae, cormophytes and animals. *Review of Palaeobotany and Palynology* **25**: 1–120. https://doi.org/10.1016/0034-6667(78)90040-4

van Geel B. 2001. Non-pollen palynomorphs. In *Tracking Environmental Change Using Lake Sediments, Terrestrial, Algal and Siliceous Indicators Vol. 3*, Smol JP, Birks HJB, Last WM (eds). Kluwer Publishers: Dordrecht; 99–119.

Vasil'ev SA, Kuzmin YV, Orlova LA *et al*. 2002. Radiocarbon-Based Chronology of the Paleolithic in Siberia and Its Relevance to the Peopling of the New World. *Radiocarbon* **44**: 503–530. https://doi.org/10.1017/S0033822200031878

Vinogradov VI, Belenitskaya GA, Pokrovsky BG *et al*. 2011. Isotopic-geochemical features of rocks of the Middle–Upper Cambrian Verkhnyaya Lena Formation in the Siberian Craton. *Lithology and Mineral Resources* **46**: 71–84. https://doi.org/10.1134/S0024490210061021

Vogel S, Märker M, Rellini I *et al*. 2016. From a stratigraphic sequence to a landscape evolution model: Late Pleistocene and Holocene volcanism, soil formation and land use in the shade of Mount Vesuvius (Italy). *Quaternary International* **394**: 155–179. https://doi.org/10.1016/j.quaint.2015.02.033

Weber AW, Jordan P, Kato H. 2013. Environmental change and cultural dynamics of Holocene hunter-gatherers in NorthEast Asia: comparative analyses and research potentials in Cis-Baikal (Siberia, Russia) and Hokkaido (Japan). *Quaternary International* **290–291**: 3–20. https://doi.org/10.1016/j.quaint.2012.07.021

Werner K, Tarasov PE, Andreev AA *et al*. 2010. A 12.5-kyr history of vegetation dynamics and mire development with evidence of Younger Dryas larch presence in the Verkhoyansk Mountains, East Siberia, Russia. *Boreas* **39**: 56–68. https://doi.org/10.1111/j.1502-3885.2009.00116.x

Willerslev E, Davison J, Moora M *et al*. 2014. Fifty thousand years of Arctic vegetation and megafaunal diet. *Nature* **506**: 47–51. https://doi.org/10.1038/nature12921

Williams JW, Tarasov P, Brewer S *et al*. 2011. Late Quaternary variations in tree cover at the northern forest-tundra ecotone. *Journal of Geophysical Research* **116**: G01017. https://doi.org/10.1029/2010JG001458

Yanase W, Abe-Ouchi A. 2007. The LGM surface climate and atmospheric circulation over East Asia and the North Pacific in the PMIP2 coupled model simulations. *Climate of the Past* **3**: 439–451. https://doi.org/10.5194/cp-3-439-2007

Zech M, Andreev A, Zech R *et al*. 2010. Quaternary vegetation changes derived from a loess-like permafrost palaeosol sequence in northeast Siberia using alkane biomarker and pollen analyses. *Boreas* **39**: 540–550. https://doi.org/10.1111/j.1502-3885.2009.00132.x

